Nano Research Energy

ISSN 2791-0091 (print); 2790-8119 (online)
https://doi.org/10.26599/NRE.2025.9120156

Review Article

# Nanoconfined iontronics and its electronic applications

Yanhui Liu[1,2,§], Puguang Peng[1,2,§], Han Qian[1,2], Zhong Lin Wang[1,3] (✉), and Di Wei[1,4] (✉)

[1] *Beijing Institute of Nanoenergy and Nanosystems, Chinese Academy of Sciences, Beijing 101400, China*
[2] *School of Nanoscience and Engineering, University of Chinese Academy of Sciences, Beijing 100049, China*
[3] *Beijing Key Laboratory of Micro-Nano Energy and Sensor, Center for High-Entropy Energy and Systems, Beijing Institute of Nanoenergy and Nanosystems, Chinese Academy of Sciences, Beijing 101400, China*
[4] *Centre for Photonic Devices and Sensors, University of Cambridge, 9 JJ Thomson Avenue, Cambridge, CB3 0FA, UK*
[§] *Yanhui Liu and Puguang Peng contributed equally to this work.*

**Received:** 26 December 2024 / **Revised:** 19 February 2025 / **Accepted:** 20 February 2025 / **Published date:** 13 March 2025

## ABSTRACT

Iontronics based on nanoconfined effects exhibit enhanced ion dynamics and have become more important in the fields such as energy harvesting and storage, sensors, and human-machine communications, which maybe an alternative or supplementary solution to electronics due to their biocompatibility and safety. The enhanced ion dynamics can be attributable to the strong interactions between ions and the electrical double layer (EDL) in the nanoconfined spaces. Therefore, in this review, an overview of the EDL is firstly provided, with its distinctive nanoconfined effects in governing ion dynamics highlighted. The primary material frameworks associated with nanoconfined spaces, including nanopores, nanochannels, and multidimensional nanostructures, are systematically classified. Strategies for modulating ion dynamics through external physical and chemical fields are explored, forming the basis for iontronic applications driven by nanoconfined effects. These applications are presented, encompassing iontronic power sources, sensors, logic components such as memristors, diodes, and transistors, as well as iontronic filter capacitors, with their unparalleled advantages in biosafety, flexibility, cost-effectiveness, and environmental adaptability emphasized. Finally, existing challenges in nanoconfined iontronics are addressed, with the expectation that advancements in nanoconfined iontronics will catalyze more efficient energy and information flow.

## KEYWORDS

nanoconfined spaces, ion transport dynamics, iontronics, applications in electronics

## 1 Introduction

Over recent decades, electronic functionality has progressed beyond basic computation and information storage to encompass a broad spectrum of intelligent applications and human-machine interactions [1]. However, as the dimensions of integrated circuits shrink to the nanoscale, traditional electronics based on the von Neumann architecture encounter critical bottlenecks in enhancing performance and minimizing power consumption, approaching the physical and practical limits of Moore's Law [2, 3]. Furthermore, while electronic signals enable efficient, rapid, and reliable transmission, conventional electronics lack the self-repair capabilities and adaptability of biological systems, rendering them vulnerable to failure in extreme environments such as intense magnetic fields, high temperatures, and high humidity [4]. Additionally, these limitations hinder the cost-effective fabrication and application of electronic systems in compact spaces. Thus, the development of novel strategies to transcend the constraints of traditional electronic devices is urgently required.

Iontronics, which has advanced significantly in recent years [5–7], leverages ions as signal or charge carriers to achieve specific functions through precise ionic regulation [8]. Biological systems, as inherently complex iontronic networks, depend on diverse ions to mediate information transmission and energy conversion, sustaining vital life processes. For instance, $Ca^{2+}$ can regulate the release of neurotransmitters in neurons [9], $K^+$ and $Na^+$ can control the transmission of synaptic electrical signals [10, 11], and $H^+$ can participate in adenosine triphosphate (ATP) synthesis within the mitochondria [12]. Inspired by biological processes, a series of biomimetic nanoconfined iontronics have been developed, including iontronic power sources [13–18], sensors [19–21], logical components of memristors [22–25], diodes [26–28], transistors [29–32] and iontronic filter capacitors [33–37]. These devices demonstrate bio-inspired attributes, including outstanding environmental adaptability, mechanical flexibility, safety, and self-healing capabilities [38, 39]. On the other hand, recent studies have revealed that the ion selectivity and transport dynamics can be significant enhanced by the overlapping of electrical double layer (EDL) at the nanoconfined



Address correspondence to Zhong Lin Wang, zhong.wang@mse.gatech.edu; Di Wei, dw344@cam.ac.uk

space, where the diameter is reduced below 100 nm [40]. Various nanoconfined materials have been successfully synthesized across different dimensions to investigate anomalous ion dynamics and their applications [41]. These include zero-dimensional (0D) nanopores (such as carbon black, silica, and molybdenum disulfide) [42–44], one-dimensional (1D) nanotubes (such as carbon nanotubes) [45, 46], two-dimensional (2D) nanoconfined materials (such as MXene, graphene oxide, carbon nitride, and metal-organic frameworks) [47–49], and three-dimensional (3D) nanoconfined hydrogels [50–52]. In addition, the introduction of external ionic regulation, via physical fields (e.g., electric fields [30, 53], light [54, 55], temperature [56, 57], and pressure [58–60]) and chemical fields (e.g., pH [61, 62], concentration gradients [63, 64], and chemical reactions [65–67]), enables precise control of ion dynamics within these nanoconfined spaces. The integration of these approaches has propelled the advancement of energy and information devices with versatile biomimetic functionalities, broadening the application scope of iontronics. Consequently, a deeper exploration of the mechanisms governing nanoconfined effects within EDL and the biomimetic regulation of ion dynamics is essential for fostering iontronic technologies with enhanced performance and superior biological adaptability.

This review begins with an overview of the evolution of EDL theory. Recent advancements in the design and fabrication of nanostructured systems utilizing diverse nanomaterials (ranging from 0D to 3D) are then summarized. Detailed attention is given to the precise regulation of ion transport behavior under external physical and chemical fields. Potential applications of iontronics in electronics are further explored, encompassing iontronic power sources, memristors, logic circuits, sensors, and filter capacitors (Fig. 1). Finally, insights and perspectives are offered on the mechanisms, stability, and durability of nanoconfined structures, alongside future directions for advancing iontronic technologies.

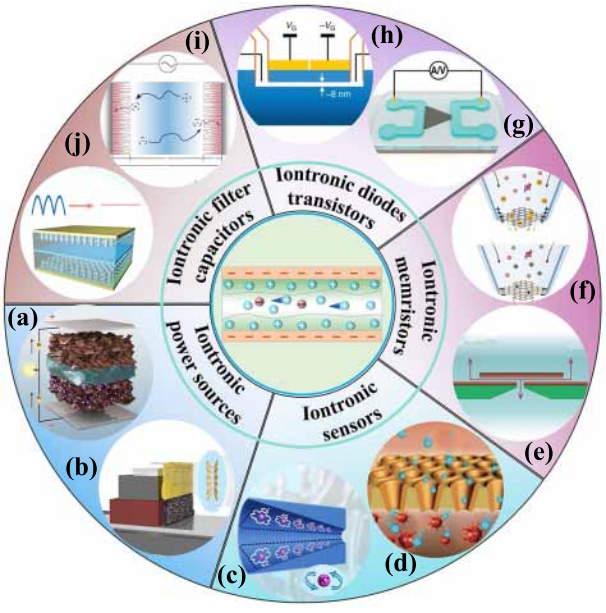


**Figure 1** Iontronics based on nanoconfined spaces with overlapped EDL, and their applications in the field of electronics. (a, b) Iontronic power sources. (a) Reproduced with permission from Ref. [15], © Wei, D. et al. 2022. (b) Reproduced with permission from Ref. [18], © Yang, F. et al. 2024. (c, d) Iontronic sensors. (c) Reproduced with permission from Ref. [68], © American Chemical Society 2015. (d) Reproduced with permission from Ref. [69], © Wiley-VCH Verlag GmbH &Co. KGaA, Weinheim 2018. (e, f) Iontronic memristors. (e) Reproduced with permission from Ref. [23], © Robin, P. et al. 2023. (f) Reproduced with permission from Ref. [70], © American Chemical Society 2024. (g, h) Iontronic diodes and transistors. (g) Reproduced with permission from Ref. [71], © Wiley-VCH GmbH 2021. (h) Reproduced with permission from Ref. [27], © Macmillan Publishers Limited 2021. (i, j) Iontronic filter capacitors. (i) Reproduced with permission from Ref. [72], © Hu, Y. et al. 2023. (j) Reproduced with permission from Ref. [73], © Elsevier Ltd. 2024.

## 2 Understanding the EDL effect in nanoconfined spaces

In nanoconfined spaces with nanopore/channel diameters smaller than 100 nm, the overlap of the EDL from the charged surface of the nanoconfined space significantly impacts ion selectivity and transport dynamics [40]. This overlapping effect can induce anomalous ion behavior within nanoconfined spaces, distinct from that in macroscopic systems [74]. Thus, a thorough understanding of the structure and properties of the EDL is essential for regulating ion dynamics, facilitating the development of high-performance systems based on nanoconfined iontronics.

### 2.1 The evolution of the EDL

The EDL model, refined over more than two centuries, serves as a foundational framework for understanding ionic-electronic coupling interfaces [5, 75, 76]. In 1853, Hermann von Helmholtz introduced the plate capacitor model of the EDL [77], proposing that contact between a conductor and a liquid creates two layers of oppositely charged ions in molecular-scale proximity to the conductor surface due to electrostatic interactions. This structure resembles a parallel-plate capacitor, with the electric potential decreasing linearly as the distance from the conductor surface increases (Fig. 2(a)). While the Helmholtz model advanced electrodynamics by characterizing charge distribution and electrochemical dynamics, it overlooks ion adsorption, diffusion, and solvent-electrode interactions, thus limiting its applicability to real solutions.

In 1910 and 1913, Gouy and Chapman independently developed the diffuse EDL model [78], addressing the limitations of the Helmholtz model. They proposed that ions near the conductor surface experience both electrostatic attraction and thermal motion, allowing them to diffuse into the bulk solution and form a diffuse layer. The ion concentration within this layer follows the Boltzmann distribution, with oppositely charged ions decreasing in concentration as the distance from the surface increases. Higher surface charges lead to more compact diffuse layers. Unlike the Helmholtz model, the potential in the diffuse layer decreases exponentially with distance (Fig. 2(b)). However, the Gouy-Chapman model does not account for electrostatic interactions and van der Waals forces between ions. In 1924, Otto Stern integrated the strengths of both the Helmholtz and Gouy-Chapman models to propose a more comprehensive EDL model [79, 80]. Stern's model accounts for the finite size of ions and van der Waals interactions. It describes the EDL as comprising a compact Stern layer, where counter-ions are strongly adsorbed onto the conductor surface, and a diffuse layer beyond it, where ions follow the distribution described by the Gouy-Chapman theory. The electric potential in the Stern layer decreases linearly with distance, while it decreases exponentially in the diffuse layer (Fig. 2(c)). Further refinements to the Stern model came from Grahame, who, in the mid-20$^{th}$ century, subdivided the Stern layer into the inner Helmholtz plane (IHP) and the outer Helmholtz plane (OHP). The IHP contains desolvated ions, while the OHP contains solvated ions. The potential decreases linearly within the IHP and exponentially in the OHP and diffuse layer. In 1963,

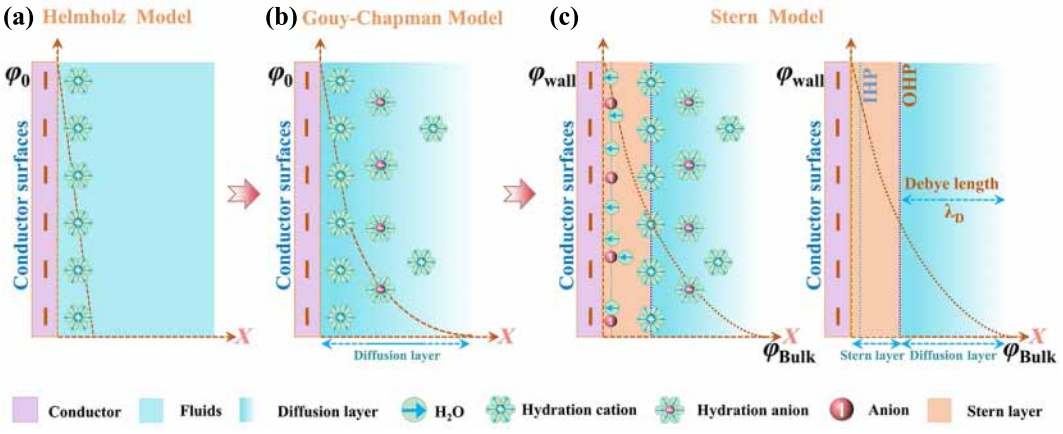


**Figure 2** The evolution of the EDL Model. (a) Helmholtz model of the EDL. (b) Gouy-Chapman model of the EDL. (c) Stern model of the EDL.

Bockris introduced an improved EDL model by incorporating the orientation of polar water molecules at the interface [81]. This model describes the IHP as including specifically adsorbed ions and ordered water molecules, while the OHP consists of solvated ions and disordered water molecules, with the diffuse layer forming the outer boundary. This model remains the most widely accepted description of the EDL today.

Together, these developments have provided a robust understanding of the EDL structure, elucidating the interplay of electrostatic forces, ion diffusion, and solvent interactions at the ionic-electronic interface.

### 2.2 EDL effect in the nanoconfined spaces

Ionic behaviors are influenced by the distinct electrochemical environments in nanoconfined spaces. To define the effective range of the EDL, the Debye length, or the thickness of the EDL, is introduced. This length typically ranges from 0.2 to 20 nm [82, 83], depending on the ion concentration and dielectric constant of the solution. The Debye length ($\lambda_D$) can be expressed as follows:

$$\lambda_D = \sqrt{\frac{\varepsilon RT}{2F^2 I_c}} \quad (1)$$

where $I_c = \frac{1}{2}\sum_i c_i z_i^2$. $\varepsilon$, $R$, $T$, $F$, and $I_c$, are the solution dielectric constant, universal gas constant, absolute temperature, Faraday constant, and ionic strength, respectively. Additionally, $c_i$ and $z_i$ are the volume concentrations and charge of the ionic species, respectively. This equation shown that the dielectric constant of the solution and the concentration of ion charges can significantly affect the Debye length of the EDL.

Ions can be significantly driven by enhanced electrostatic interactions when within this range, resulting in anomalous ion dynamics. Particularly in nanoconfined spaces, the role of the EDL becomes critical due to its overlap. Shown in Fig. 3, as the diameter of the nanoconfined space decreases below 100 nm [84], the electrostatic repulsion or attraction effects from the overlapped EDL can effectively select specific ions and regulate overall ion dynamics. In sub-nanoconfined spaces (diameter < 2 nm), hydration and weak intermolecular forces (such as hydrogen bonding and van der Waals interactions) play a crucial role in ion regulation, which leads to a series of anomalous ion behaviors, including ion Coulombic blocking [85], superionic states [86], drastic changes in diffusion coefficients [87], ion-ion correlations [88], and ultra-dense packing of ions [89–91], etc. The EDL effects in nanoconfined spaces hold profound scientific significance and considerable application potential in seawater separation [92], ion screening [93, 94], and nanosensors [95, 96], among others. In energy harvesting and storage devices, these effects can enhance ion flux and conductivity, thereby improving performance and energy conversion efficiency.

## 3 Nanoconfined materials

The development of the EDL model and its special effects in nanoconfined spaces has further leaded the improvement of nanoconfined materials, which can be the key component to the multifunctional and high-performance iontronics. Therefore, a deep understanding of the design, fabrication, and application of nanoconfined materials, spanning 0D to 3D, is crucial for elucidating the relationship between nanoconfined ion dynamics and iontronics, as well as for highlighting the advantages of iontronics over traditional electronics (Fig. 4).

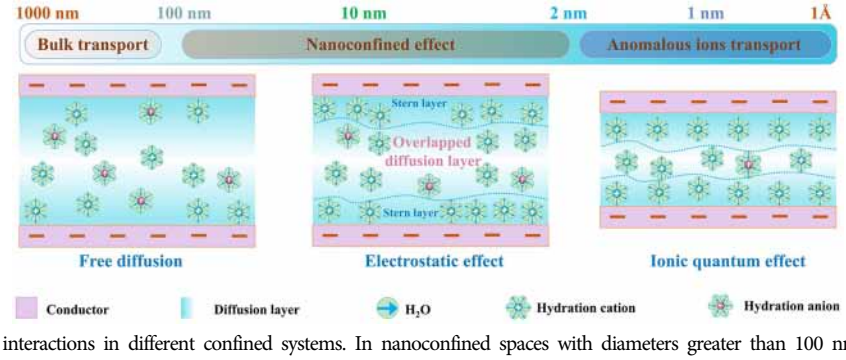


**Figure 3** Schematic of ion interactions in different confined systems. In nanoconfined spaces with diameters greater than 100 nm, ions exhibit free diffusion characteristics. In the 2 to 100 nm range, ion transport is governed by the EDL. In sub-nanometer spaces with diameters smaller than 2 nm, anomalous ion transport behaviors are observed.

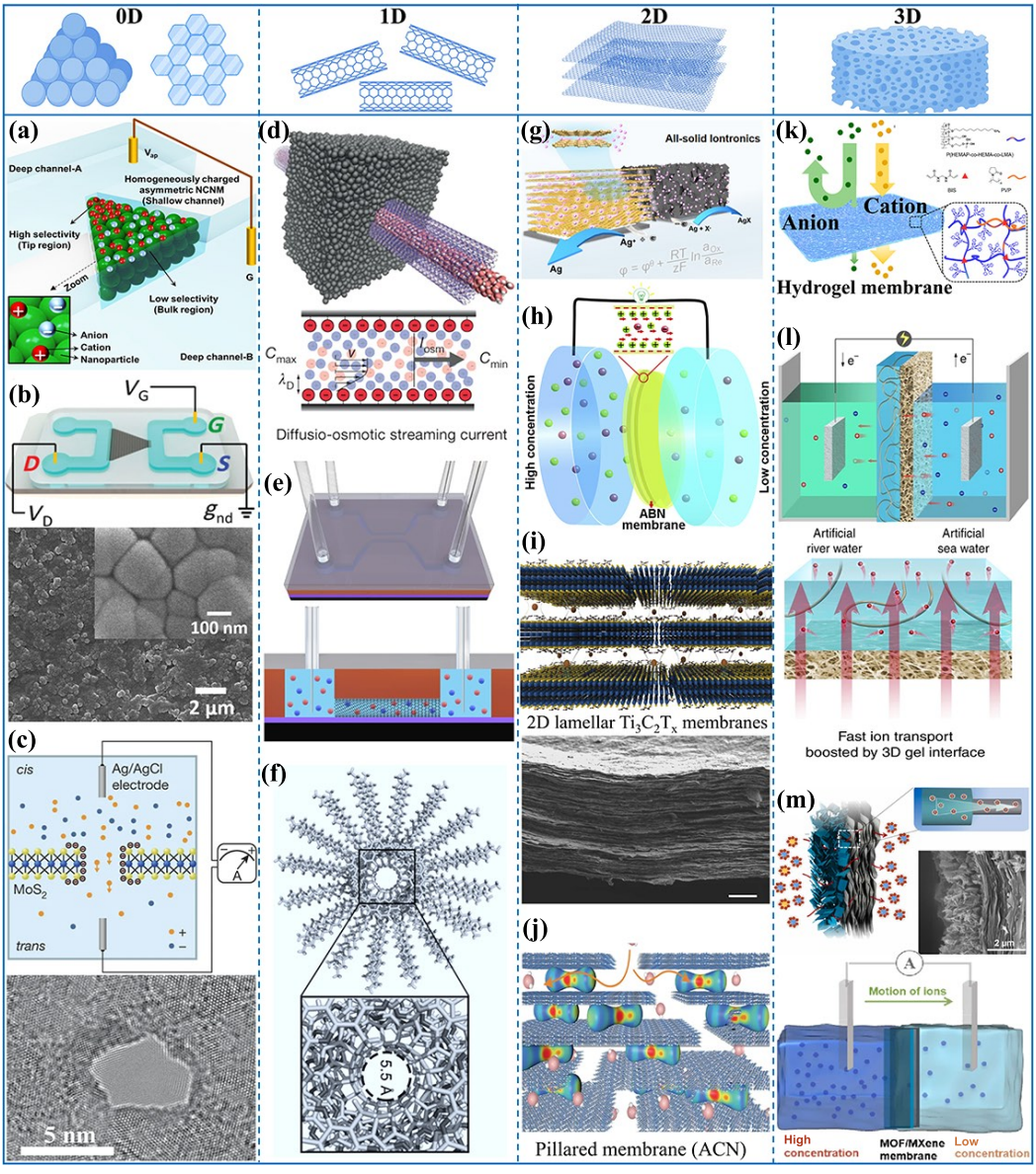


**Figure 4** Summary of nanoconfined materials from 0D to 3D. (a) Schematic diagram for the current iontronic diode based on asymmetric $SiO_2$ nanopore networks membrane. Reproduced with permission from Ref. [97], © American Chemical Society 2016. (b) Iontronic diodes based on an asymmetric-shaped carbon black nanoparticle membrane. Reproduced with permission from Ref. [71], © Wiley-VCH GmbH 2021. (c) Schematic illustration of an osmotic energy harvester based on single-pore $MoS_2$. Reproduced with permission from Ref. [44], © Macmillan Publishers Limited 2015. (d) Schematic diagram an osmotic energy harvesting device based on single BNNTs. Reproduced with permission from Ref. [45], © Macmillan Publishers Limited 2013. (e) Schematic diagram of an osmotic energy harvesting device based on DWCNTs. Reproduced with permission from Ref. [46], © Cui, G. et al. 2023. (f) Schematic of nanoconfined channels formed by pore-containing hydrazide helical macromolecules. Reproduced with permission from Ref. [98], © Wiley-VCH Verlag GmbH &Co. KGaA, Weinheim 2016. (g) Iontronic power sources based on 2D layered GO. Reproduced with permission from Ref. [17], © Elsevier Ltd. 2024. (h) Schematic diagram of osmotic energy harvesting based on the ABN membrane. Reproduced with permission from Ref. [47], © Elsevier Ltd. 2020. (i) Schematic illustration of the 2D lamellar $Ti_3C_2T_x$ alginate membranes. Reproduced with permission from Ref. [99], © Wang, J. et al. 2020. (j) Schematic diagram of carbon nitrides membrane modified with stabilizers. Reproduced with permission from Ref. [100], © Wang, Y. et al. 2022. (k) Schematic illustration 3D interconnected structures of hydrogel membranes. Reproduced with permission from Ref. [52], © American Chemical Society 2020. (l) Schematic of 3D polyelectrolyte hydrogel heterogeneous membrane. Reproduced with permission from Ref. [50], © Zhang, Z. et al. 2020. (m) Schematic diagram of the 3D heterostructure based on the combination of MOF and MXene. Reproduced with permission from Ref. [101], © Elsevier Ltd. 2024.

### 3.1 Iontronics based on 0D nanopores

0D nanopores can be obtained from selective etching of membranes or interconnected voids that formed between nanoparticles through self-assembly methods. In recent years, representative 0D nanomaterials such as single-pore graphene [102, 103], silica ($SiO_2$) [97], alumina ($Al_2O_3$) [42, 104], carbon black [71, 105], and single-pore molybdenum disulfide ($MoS_2$) [44, 106, 107] have been extensively employed in the fabrication of nanoconfined spaces. Additionally, the edges of nanopores can be precisely functionalized with specific groups to regulate surface EDL, which offers a flexible approach to designing multifunctional 0D nanomaterials. Currently, nanoconfined structures developed from nanopores with tunable surfaces are widely employed in applications such as molecular sieving, desalination, biosensors, and iontronic diodes, showing an enhanced performance compared with traditional membranes and devices [108–111].

In detail, asymmetric and conical nanoconfined structures can

be created by densely packing negatively charged silica nanoparticles, ideal for diode applications that require high ionic current and rectification ratios (Fig. 4(a)) [97]. When the narrow end of a conical pore approaches the Debye length, it exhibits exceptional ion selectivity. In a 1 mM potassium chloride (KCl) solution, applying a positive voltage enhances the ionic current, while a negative voltage dissipates $K^+$ ions within the pores, reducing the current to negligible levels. This straightforward packing approach overcomes challenges such as high fabrication costs, low ionic currents, and limited ion transport mechanisms. Similar structures have been developed using materials like carbon black and $Al_2O_3$ nanoparticles. For example, a membrane formed from carbon black nanoparticles with pore gaps smaller than 10 nm significantly enhances cation selectivity (Fig. 4(b)) [71]. Introducing asymmetry and reconstructing surface charge polarity in these nanoconfined spaces increases the rectification ratio of ionic diodes by up to 30-fold. In addition, 0D nanomaterials can also be employed in osmotic power harvesting. A standard silicon micromachining process assembles dispersed negatively charged silica nanoparticles into $SiO_2$ nanoconfined membranes with face-centered cubic structures [42]. Exposing these $SiO_2$ nanoconfined membranes to KCl solutions with varying concentrations creates nanoconfined spaces where the Debye length ranges from 1 to 30 nm. The diffusion of $K^+$ ions across the concentration gradient, coupled with overlapping EDL effects, generates an electric current. Reducing nanopore diameters intensifies EDL overlap, thereby further enhancing conductivity and power output. This precise modulation of ion dynamics provides a highly effective strategy for energy harvesting. Moreover, single-layer $MoS_2$ nanopores with 5 nm diameter, fabricated using atomic-level electrochemical reaction (ECR) techniques or electron irradiation under transmission electron microscopy (TEM), facilitate salinity gradient conversion (Fig. 4(c)) [44]. When the $MoS_2$ nanopore membrane is placed in solutions of different concentrations of KCl, the chemical potential gradient and the EDL overlapped effect within the nanoconfined space drive the rapid transport of $K^+$ ions through the nanopores, generating an ionic current. As the concentration gradient increases, the diffusive ionic current becomes stronger. Theoretically, the power density of the osmotic power generator, based on EDL-enhanced cation selectivity and the salinity gradient effect, can reach up to $10^6$ $W \cdot m^{-2}$.

### 3.2 Iontronics based on 1D nanoconfined materials

1D nanomaterials generally refer to nanomaterials with nanometer-scale diameters, where the length substantially exceeds the cross-sectional dimensions. In recent years, various 1D nanomaterials, such as carbon nanotubes (CNTs) and boron nitride nanotubes (BNNTs), have been extensively used to construct nanoconfined spaces. Due to their unique properties, such as tunable surface functional groups, high surface area, stretchability, ease of fabrication, and exceptional resistance to damage, 1D nanomaterials have found applications in iontronics, including energy harvesting and storage, seawater desalination, sensors, and drug delivery.

For instance, BNNTs with radii between 15–40 nm were embedded in silicon nitride films using an electric field ion evaporation method [45], connecting two reservoirs with different KCl salinity gradients (Fig. 4(d)). Due to their high sensitivity to pH variations, BNNTs enable modulation of surface charge density within nanoconfined spaces by adjusting the solution's pH, thereby enhancing the overlap of EDL. This EDL effect accelerates $K^+$ ion transport, generating a power density of 4 $kW \cdot m^{-2}$. Similarly, Ma et al. fabricated a single double-walled carbon nanotube (DWCNT) with an inner radius of 2.3 nm using photolithography for osmotic power conversion (Fig. 4(e)) [46]. When exposed to reservoirs with different concentration gradients, the performance varied depending on the degree of EDL overlapped. Under enhanced EDL effects, $K^+$ ions rapidly transport through the negatively charged nanoconfined space. This DWCNT-based osmotic power conversion device achieves a power density of 22.5 $kW \cdot m^{-2}$ when the concentration gradient differs by a factor of 1000. Such precisely controlled 1D nanoconfined structures are promising candidates for osmotic power harvesting under salinity gradients. Additionally, a single-molecule nanoconfined channel was developed using linear hydrazide macromolecules as precursors via pre-polymerization (Fig. 4(f)) [98]. The resulting 1D channel, with a diameter of 0.55 nm, features a stable pore structure supported by helical polymer scaffolds. This structure offers collapsibility, extended channel lifetime, and efficient cation transport, comparable to natural protein channels.

### 3.3 Iontronics based on 2D nanoconfined materials

2D nanomaterials, including graphene oxide (GO), $MoS_2$, MXenes, and boron nitride (BN) etc. have become the central part to the study of ion dynamics within 2D nanoconfined spaces. These materials possess several key attributes that make them indispensable for diverse applications, including active surfaces, flexibility, stability, and tunable channel heights. The high specific surface area of 2D materials, combined with their adjustable surface functionality, activates reactive sites to significantly enhance ion selectivity within nanoconfined channels, enabling precise ionic transport control. Their exceptional mechanical properties, such as flexibility and resilience under bending, stretching, and compression, ensure stable performance under dynamic conditions, making them integral to flexible electronics, advanced sensors, and wearable devices. Furthermore, their outstanding chemical and thermal stability under extreme conditions, including high temperatures and corrosive environments, ensures long-term reliability and minimizes maintenance requirements. The ability to modulate interlayer spacing with nanometer precision further provides unparalleled selectivity for specific ions and molecules, advancing applications in molecular separation, ion regulation, and filtration technologies. Collectively, these attributes position 2D materials as versatile platforms for the development of next-generation iontronic devices and sustainable technologies.

More importantly, 2D nanomaterials exhibit excellent self-assembly and printability, enabling large-area, scalable fabrication and broad applicability. For example, Wei et al. developed an iontronic power source using printed GO (Fig. 4(g)) [17]. The GO channels, printed on flexible substrates, exhibit a height of only 5.5 Å, which enhances EDL effects within the nanoconfined spaces. Lithium ions ($Li^+$) in reduced graphene oxide rapidly transport through these negatively charged channels under a concentration gradient, generating high power and energy densities. Furthermore, printing GO on polyethylene terephthalate (PET) substrates facilitates the development of compact iontronic power sources, offering potential for miniaturized energy harvesting and storage devices. In addition, BN membranes are also promising for osmotic power generation due to their stability. Aramid-boron nitride (ABN) composite membranes, fabricated through layer-by-layer assembly of BN nanosheets and aramid nanofibers, exhibit tightly stacked, highly hydroxylated surfaces (Fig. 4(h)) [47]. These surfaces are highly sensitive to pH

variations, which modulate EDL overlapped effects and promote rapid cation transport through the negatively charged nanoconfined spaces. This ABN-based system achieves a power density of 0.6 $W \cdot m^{-2}$ by precisely controlling ionic transport.

On the other hand, MXenes, 2D transition metal carbides and/or nitrides, are emerging as critical materials for energy harvesting, ion sieving, and biosensing. Among them, titanium carbide ($Ti_3C_2T_x$) stands out due to its mechanical robustness and stability in aqueous environments. Wang et al. stabilized the nanoconfined structure of $Ti_3C_2T_x$ membranes by incorporating alginate hydrogel columns (Fig. 4(i)) [99]. These columns maintain a consistent interlayer spacing of ~7.4±0.2 Å, enabling efficient monovalent cation transport and sustaining ion sieving performance for up to a month. Additionally, Wei et al. developed horizontally aligned MXene (H-MXene) membranes for ionic sequential transport and permeation energy harvesting [112]. The H-MXene membranes exhibit excellent cation selectivity influenced by concentration gradients and EDL effects, achieving an osmotic power density of 9.47 $W \cdot m^{-2}$ and an energy conversion efficiency of 45.7%.

Polymeric carbon nitride (CN, also known as g-$C_3N_4$) has also attracted attention for its semiconductor properties and resistance to interlayer expansion in solution environments. Antonietti et al. constructed sub-nanoconfined CN channels with widths below 6 Å using braced structure (Fig. 4(j)) [100]. These materials create rigid, interlocked structures that exhibit exceptional water stability and resistance to swelling. Under the influence of EDL effects, monovalent cations preferentially traverse nanoconfined spaces, while multivalent cations are excluded through size-selective mechanisms. Further reduction in layer spacing enables CN membranes to achieve efficient desalination, permitting water molecules to pass while effectively rejecting ions.

### 3.4 Iontronics based on 3D nanoconfined materials

3D nanomaterials, characterized by nanostructures ranging from 1 to 100 nm in all spatial dimensions, include notable examples such as hydrogels and heterostructured assemblies. In iontronics, 3D nanoconfined materials present distinct advantages over their 2D counterparts. Their intricate architectures offer significantly higher specific surface areas, enhancing ion interactions and markedly improving energy conversion efficiency. The precise tunability of channel structures in 3D materials facilitates selective ion filtration based on valence, a critical feature for advancing system efficiency and purity in sophisticated filtration technologies. The high-density networks of nanopores or nanochannels intrinsic to 3D nanomaterials provide extensive pathways for ion regulation and transport, boosting ion flux and optimizing adsorption and diffusion processes essential for high-performance ionic devices. Additionally, 3D nanoconfined materials exhibit superior structural stability and mechanical resilience, ensuring reliable performance under extreme environmental conditions. These attributes position 3D self-assembled heterojunction membranes as highly promising candidates for next-generation applications, including advanced filtration systems, precision sensing platforms, and efficient desalination technologies.

For instance, Wen et al. fabricated a hydrogel membrane using 2-hydroxyethyl methacrylate phosphate (HEMAP) through photopolymerization (Fig. 4(k)) [52]. The resulting membrane features a negatively charged surface with interconnected nanopores averaging 5.4 nm in diameter. This structure induces overlapped EDL within the nanopores, enhancing cation transport dynamics. When subjected to a 50-fold KCl salinity gradient, the HEMAP hydrogel-based osmotic power source delivered an output power of 5.38 $W \cdot m^{-2}$. The charge-controlled ion transport in this system positively correlates with the charge density within the nanoconfined space. The 3D interconnected structure and distributed charges significantly enhance the hydrogel membrane's osmotic power performance. The synergistic effects of asymmetry, charge distribution, and wettability in heterojunction membranes further introduce unique ion transport properties, such as the ion diode effect. This unidirectional ion transport minimizes Gibbs free energy dissipation as Joule heat, improving membrane performance. Jiang et al. developed a 3D hydrogel interface for osmotic power conversion (Fig. 4(l)), consisting of a polyelectrolyte hydrogel layer supported by a porous aromatic polyamide nanofiber (ANF) membrane [50]. The ANF membrane, with nanopores between 5 and 10 nm, carries a negative charge, while the hydrogel layer has a higher surface charge density and 12 nm nanopores. In a seawater/river-water reservoir, overlapping EDL effects in the ANF membrane preferentially facilitate $Na^+$ transport through the nanoconfined space. The negative charge networks and wider transport pathways in the hydrogel layer enable unidirectional $Na^+$ transport, enhancing transmembrane ionic current and interface transfer efficiency. This design achieves a power output of 5.06 $W \cdot m^{-2}$, showcasing potential for energy-harvesting iontronic applications. Similarly, an asymmetric metal-organic framework (MOF)/MXene heterostructure was synthesized via electrochemical deposition of MOF onto MXene (Fig. 4(m)) [101]. The resulting channels have diameters of 17.51 and 4.34 nm, respectively. Both the hierarchical structure of MXene and the negatively charged MOF surfaces create EDL-enhanced nanoconfined spaces, improving ion permeability and cation selectivity. The optimized porous membrane exhibits a cation selectivity of 0.95 and a power density of 35.04 $W \cdot m^{-2}$. This heterostructure design enhances osmotic power generation and holds promise for applications in gas separation, ion sieving, desalination, and logic circuits.

## 4 External field enhanced ion dynamics for iontronics

Iontronic performance can be modulated by controlling the geometry and surface charge density of nanoconfined spaces, as well as by introducing external physical fields (e.g., electric fields, light, heat, pressure) and chemical fields (e.g., pH and concentration gradients). These external fields can enhance ion transport dynamics within nanoconfined spaces, mirroring the ion regulation mechanisms prevalent in biological systems. By leveraging these effects, various biomimetic energy conversion and information transmission devices have been developed, greatly expanding the potential applications of iontronics.

### 4.1 Ion dynamics enhanced by external electric fields

External electric field-enhanced ion dynamics involve the modulation of ion migration, diffusion, and behavior within nanoconfined spaces under applied electric fields. The electric field induces directional ion migration, accelerating diffusion, altering transport pathways, and influencing interfacial chemical reaction rates. This mechanism enhances ion mobility, modulates nanoscale ionic currents and conductivity, and optimizes the performance of iontronic devices. Key principles include electrostatic field enhancement, field-effect modulation, and electric-field-driven ion separation [71, 113, 114], which lead to

ion migration by electrostatic interactions or extra electric field forces. These effects underpin diverse applications in energy storage, sensors, iontronic signal processing, water treatment, and wearable electronics.

Recent studies demonstrate that voltage can effectively regulate ion selectivity in ionic diodes. This selectivity is readily observed through ionic current rectification in current-voltage (*I-V*) measurements. Azzaroni et al. fabricated solid-state conical nanopores coated with a conductive poly(3,4-ethylene-dioxythiophene) (PEDOT) layer using etching and chemical synthesis methods (Fig. 5(a)). The PEDOT layer acts as a non-metallic gate electrode. Applying different voltages alters both the electrochemical state of PEDOT and the nanopore's surface charge, enabling precise control over the direction and magnitude of ionic currents. In the oxidized (p-doped) state, the *I-V* curve is linear when a gate voltage of $V_g$ = –0.2 V is applied, indicating electrical neutrality with no rectification. Further reduction (n-doping) at $V_g$ < –0.2 V induces negative rectification, enhancing cation selectivity. In contrast, oxidation or p-doping increases positive rectification, enhancing anion selectivity. Excessive oxidation ($V_g$ > 0.8 V) degrades the film, highlighting the need for careful voltage control to achieve high rectification ratios [115]. Additionally, MXene nanosheets assembled into layered membranes with sub-nanometer interlayer channels exhibit voltage-gated ion transport properties (Fig. 5(b)) [116]. Without an external voltage, $K^+$ ions traverse the channels under the influence of concentration gradients and overlapping EDL, generating osmotic power. Applying a negative gate voltage increases the negative potential within the nanoconfined spaces, enhancing cation-surface interactions and reducing ionic conductivity. Conversely, a positive gate voltage neutralizes surface charges, increasing ionic conductivity. This voltage-controlled regulation of ion dynamics offers an effective strategy for improving ion exchange membranes, osmotic power conversion, and molecular filtration.

The enhancement of ion dynamics and its precise control by external electric fields within nanoconfined spaces not only optimizes processes such as energy conversion, ion sieving, and diode rectification but also lays a solid theoretical and experimental groundwork for designing iontronic systems with advanced and versatile functionalities.

### 4.2 Ion dynamics enhanced by light

Light, characterized by its abundance, safety, cost-effectiveness, and broad availability, has emerged as a pivotal tool for regulating ion transport. Light-enhanced ion dynamics involve the modulation of ion behavior within nanostructures through parameters such as intensity, wavelength, and frequency. This process leverages light-induced surface charge redistribution to facilitate ion migration. Photosensitive materials play a crucial role, enabling photoelectric, photochemical effects that accelerate ion motion, induce photochemical reactions, or adjust surface charge density for selective ion transport. Key mechanisms include photoelectric effects [117–119] or photochemical reactions [65] that generate photoinduced potentials for ion migration, finding extensive applications in photocatalysis, solar energy harvesting, light-controlled sensors, photo-driven intelligent systems, and biosensing technologies.

Wei et al. reported a direct current triboelectric nanogenerator (DC-TENG) that utilizes ionic currents from reduced graphene oxide (rGO)/GO junction for TENG rectification (Fig. 6(a)). However, during the contact separation process of DC-TENG, the $K^+$ concentration gradient in the rGO/GO junction will decrease, which makes the rectification gradually ineffective. Herein, ultraviolet light can be used to charge the junction. When the rGO side is irradiated with ultraviolet light, electron-hole pair separation occurs within the rGO, which leads to the generation of a built-in electric field within the rGO/GO junction. Therefore, the built-in electric field facilitates the rapid transport of $K^+$ ions within the GO nanoconfined space, which significantly enhancing the ionic current and thereby improving the DC output performance of the DC-TENG [119]. Additionally, tungsten disulfide ($WS_2$) composite membranes demonstrate efficient osmotic power conversion due to their superior photo-responsive

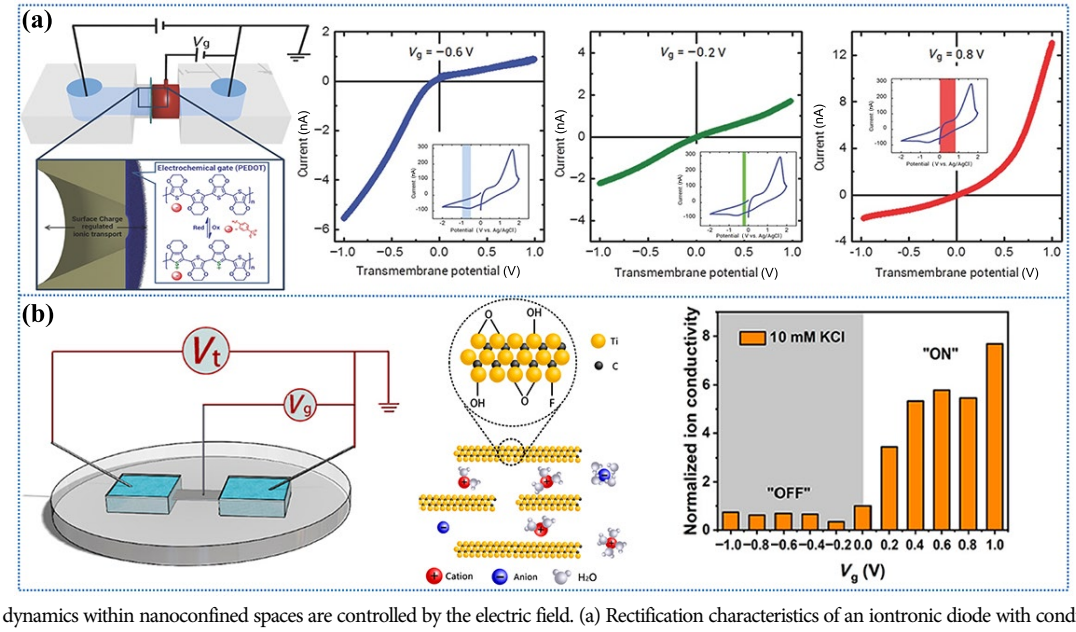


**Figure 5** Ion dynamics within nanoconfined spaces are controlled by the electric field. (a) Rectification characteristics of an iontronic diode with conductive polymers (PEDOT) as the gate electrode under varying gate voltages. Reproduced with permission from Ref. [115], © WILEY-VCH Verlag GmbH & Co. KGaA, Weinheim 2017. (b) The MXene membrane was placed in the reservoir. Subsequently, ion dynamics within the membrane being modulated via the gate voltage. Reproduced with permission from Ref. [116], © American Chemical Society 2019.

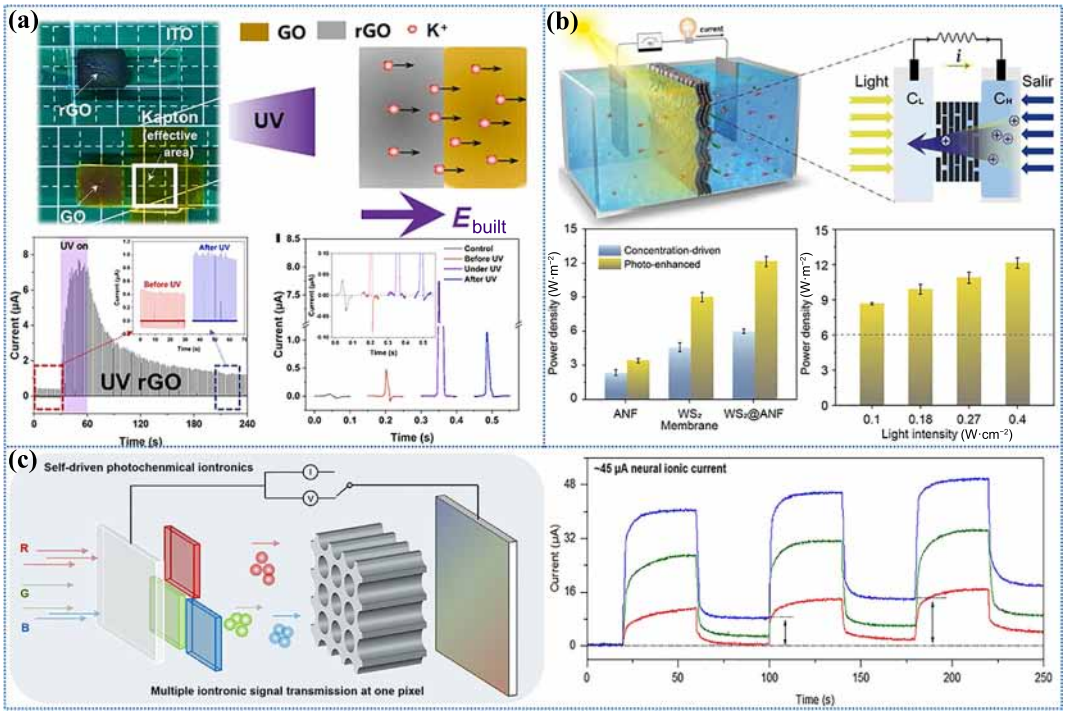


**Figure 6** Ion dynamics within nanoconfined spaces are controlled by light. (a) The light-enhanced ionic current in the rGO/GO junction is used for rectification in the TENG. Reproduced with permission from Ref. [119], © Elsevier Ltd. 2023. (b) Schematic of ion transport in the $WS_2$ composite membrane and energy conversion in the photo-enhanced composite membrane. Reproduced with permission from Ref. [120], © Wiley-VCH GmbH 2023. (c) Anion transport in silver halides (AgX, where X = $Cl^-$, $Br^-$, or $I^-$) in AAO membranes is affected by light drive. Reproduced with permission from Ref. [65], © Elsevier Ltd. 2024.

properties. When illuminated on the low-concentration side of the reservoir (Fig. 6(b)) [120], the $WS_2$ membrane exhibited enhanced output current and osmotic power. Asymmetric illumination induces a high negative surface charge density and concentration gradient, increasing cation selectivity and ion flux within the nanoconfined spaces. Under illumination, the power output from mixing seawater and river water reached 16.43 $W{\cdot}m^{-2}$. Photothermal and photovoltaic effects in such materials have significantly improved osmotic power conversion efficiency. Further innovations include a monolayer iontronic retinal array constructed using nanoporous anodic aluminum oxide (AAO) (Fig. 6(c)) [65]. Silver halides (AgX, where X = $Cl^-$, $Br^-$, or $I^-$) serve as carriers of different types of light. Light-triggered anion transport within the positively charged AAO nanoconfined spaces generates distinct photovoltage and photocurrent signals, enabling color recognition and integrating sensing, information processing, and storage functions within a single pixel.

The ability of light to modulate ion dynamics within nanoconfined spaces presents exceptional potential for advancing iontronic applications. Through the strategic use of light, significant enhancements in performance and sensitivity can be achieved across a range of technologies, including energy harvesting, energy storage, sensing, and ion sieving.

### 4.3 Ion dynamics enhanced by heat

Heat-enhanced ion dynamics involves the regulation of ion transport within nanoconfined spaces through temperature variations. This includes thermal diffusion effects and the temperature-driven acceleration of ion dynamics, such as the Soret effect and photothermal effect. Higher temperatures increase ionic thermal motion by modifying ionic diffusion coefficients and conductivity, thereby improving diffusion rates and transport efficiency within nanoconfined channels. This phenomenon is widely applied in thermoelectric power generation, thermal sensors, energy storage systems, wearable devices, and temperature-responsive materials.

Building on this concept, Su et al. developed conical nanopores in PET using an asymmetric etching method. By integrating silica nanopores prepared through a solution growth technique, they formed SIM/PET hybrid nanochannels (Fig. 7(a)) [56]. These hybrid nanochannels feature negatively charged surfaces and exhibit cationic permselectivity, enabling the detection of diffusion potential differences across the channels. When a small temperature gradient is applied, the system demonstrates a highly sensitive thermoelectric response, with a sensitivity of 0.71 $mV{\cdot}K^{-1}$, comparable to natural thermal sensing systems. Additionally, the hybrid nanochannels exhibit rapid response to temperature changes, with a relative response speed exceeding 98%. This thermosensitive ion-channel-based biosensing system holds potential for applications in detection and thermoelectric energy conversion. A thermoelectric conversion system based on covalent organic frameworks (COFs) was also introduced (Fig. 7(b)) [121]. COF membranes can intelligently monitor temperature changes and generate continuous potential differences in response. This thermoelectric conversion system can exhibit different directional ion transport behaviors under hot and cold conditions. Moreover, these membranes demonstrate consistent transmembrane diffusion potential differences across a broad range of ion concentrations and temperatures, attributed to enhanced EDL overlapped effects and high surface charge densities. Thermal modulation provides precise control over ion transport dynamics within nanoconfined spaces, facilitating the development of smart textiles with heat-sensing capabilities. Real-time electrical output responses demonstrate the high sensitivity of these iontronic sensors. Additionally, Liu et al. fabricated hierarchical graphene foam (H-G foam) with continuous pores on a nickel foam

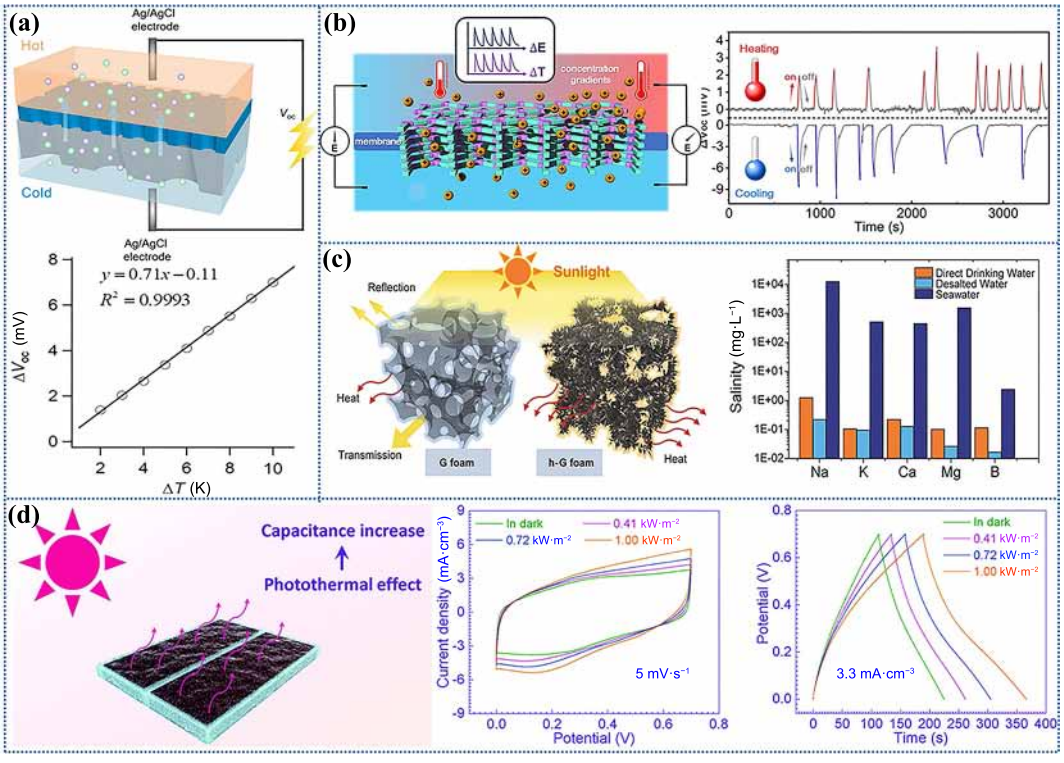


**Figure 7** Ion dynamics within nanoconfined spaces are controlled by heat. (a) Thermoelectric response of the hybrid nanochannel SIM/PET under different temperature gradients. Reproduced with permission from Ref. [56], © American Chemical Society 2019. (b) Thermal-responsive system based on 2D covalent organic framework membranes. Reproduced with permission from Ref. [121], © Zhang, P et al. 2021. (c) H-G foam is used for solar–vapor desalination. Reproduced with permission from Ref. [122], © WILEY-VCH Verlag GmbH & Co. KGaA, Weinheim 2017. (d) H-G foam with excellent photothermal properties for improving the performance of supercapacitors. Reproduced with permission from Ref. [123], © The Royal Society of Chemistry 2018.

substrate using plasma-enhanced chemical vapor deposition (Fig. 7(c)). Under illumination, this H-G foam exhibits a photothermal energy conversion efficiency of approximately 93.4%. More importantly, the unique foam network structure of H-G foam gives it exceptional seawater desalination capabilities [122]. Water filtered through H-G foam can be directly consumed as drinking water. The excellent photothermal properties of H-G foam also make it a promising material for energy storage applications. Wei et al. developed a supercapacitor using three-dimensional H-G foam as the electrode material (Fig. 7(d)). Photothermal energy enhances ion dynamics within the electrolyte, facilitating ion transport and adsorption in the porous H-G foam, which in turn boosts the ionic current. The supercapacitor exhibits higher current density and longer discharge time when the light intensity increased. As a result, the supercapacitor's capacitance, energy density, and power density are significantly improved with the increasing light intensity [123].

Heat modulation offers an efficient means to enhance ion transport within nanoconfined spaces, enabling the realization of specific functionalities. As a result, thermosensitive and photothermal materials have attracted significant research attention. The thermal regulation of ion dynamics in these spaces presents new strategies for optimizing energy harvesting, environmental monitoring, seawater desalination, and advancing iontronic sensor technologies.

### 4.4 Ion dynamics enhanced by pressure

Pressure serves as another physical method for regulating ion dynamics within nanoconfined spaces, involving the control of ion and molecule transport through external pressure application. The geometry of the nanoconfined space changes under pressure, leading to variations in ionic transport pathways and mobility. This approach has found applications in high-pressure sensors, gas separation, chemical reaction control, and piezoelectric energy harvesting.

For instance, Jiang et al. developed an iontronic sensor using a layered graphene hydrogel membrane (GHM) (Fig. 8(a)) [58]. In humid conditions, 2D nanocapillaries form between adjacent graphene sheets. When electrolyte flows through the GHM under external mechanical force, a synchronous ionic current is generated. The GHM acts as an effective charge filter, where increasing pressure allows more cations to traverse the nanoconfined spaces, thereby enhancing ionic current and conductivity. This sensor can produce continuous and pulsatile ionic current signals in real time, reflecting the input waveform of the mechanical force. The enhanced EDL overlapped effects enable precise ion regulation. Furthermore, such iontronic sensors can harvest electrical energy from footfalls and body fluid flow or monitor heartbeats, emulating biological mechano-transduction, where membrane deformation initiates $Na^+$ ion flow and generates action potentials. Inspired by such biological processes, Han et al. developed a biomimetic iontronic pressure sensor composed of stacked polymers, electrolytes, and nanopore membranes (Fig. 8(b)) [124]. A silicone tape with a 2 cm ×1.5 cm hole is affixed to a polyvinylidene fluoride (PVDF) support, and polyaniline (PANi) electrolyte is introduced into the hole. An etched polycarbonate (PCTE) membrane is then positioned between two electrolyte reservoirs. The resulting sensor exhibits a sensitivity of ~5.6 $kPa^{-1}$, a response time of ~12 ms, and operates at 1 Hz with power consumption under a few μW. In addition, with the increase in pressure, the ion transport speed within the nanoconfined structure is also accelerated, leading to a higher ionic current. Reliability tests confirm stability over 10,000 loading-

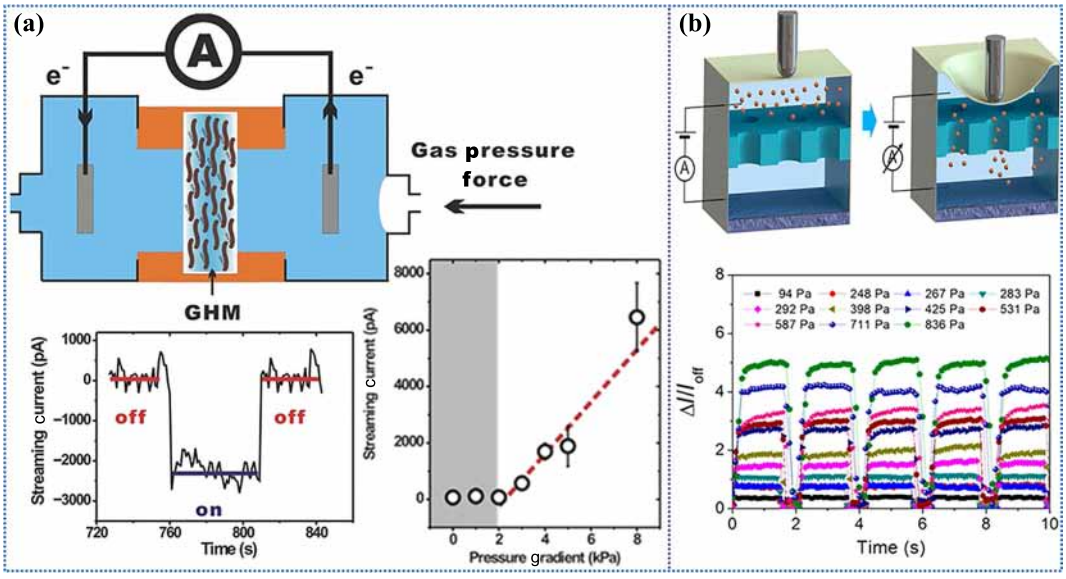


**Figure 8** Ion dynamics within nanoconfined spaces are controlled by pressure. (a) Iontronic sensors based on a layered graphene hydrogel membrane. Reproduced with permission from Ref. [58], © WILEY-VCH Verlag GmbH & Co. KGaA, Weinheim 2013. (b) Current variation curve of the biomimetic iontronic sensor under different pressures. Reproduced with permission from Ref. [124], © American Chemical Society 2016.

unloading cycles. This sensor effectively monitors human blood pressure and pulse, capturing distinct physiological signals. In the future, such iontronic mechanoreceptors could be integrated into robotic hands for tactile sensing, enhancing environmental interactions.

In summary, pressure-driven modulation of ion dynamics in nanoconfined spaces facilitates a wide range of applications in energy harvesting, storage, sensing, seawater desalination, and biomedicine. This approach offers both theoretical insights and practical strategies for the development of advanced, high-efficiency iontronic devices.

### 4.5 Ion dynamics enhanced by pH

pH-enhanced ion dynamics involve modulating ion behavior in nanoconfined spaces by adjusting the solution's acidity or alkalinity. pH variations influence surface charge density, thereby affecting ion adsorption, diffusion, and transport. By altering the ionic charge state, pH adjustments control ion migration pathways and velocities, optimizing ion selectivity and dynamic performance. This mechanism is crucial for improving energy harvesting, ion sieving, sensor sensitivity, and desalination efficiency.

The surface charge of nanoconfined channels is highly responsive to pH variations, directly affecting ion dynamics. Xu et al. achieved the interface growth of a COF ($TpBDMe_2$) on AAO (Fig. 9(a)) [125]. They observed a significant increase in the permeation rate of $K^+$ within the pH range of 2.6 to 4.6, corresponding to the isoelectric point, and a gradual increase between pH 4.6 and 6.0. This behavior correlates with the zeta potential of the channel surface: at lower pH values, the positively charged channel repels cations, hindering $K^+$ transport. Conversely, at higher pH values, the negatively charged channel attracts cations, enhancing $K^+$ transport and increasing $K^+/Mg^{2+}$ selectivity from $10^2$ to $10^3$. By tuning the pH of the electrolyte, ion transport dynamics within membrane channels can be precisely regulated, facilitating efficient ion sieving. This property has led to the development of various salt-alkali-resistant nanoconfined membranes. pH regulation also enhances the rectification ratio of iontronic diodes. For example, aluminum oxide ($Al_2O_3$) nanopore arrays partially modified with polypyrrole (PPy) layers form an organic/inorganic hybrid nanoconfined structure [126]. By adjusting the solution's pH, the surface charge density and polarity within the asymmetric nanoconfined space can be modulated, creating discontinuous charge distributions. This behavior promotes the preferential transport of $Na^+$ or $Cl^-$, resulting in pH-responsive ionic rectification (Fig. 9(b)). Similarly, a 3D polyphenylsulfone membrane with pyridine side chains exhibits reversible changes in surface charge density and polarity under precise pH control [127]. The surface of the modified membrane carries a positive charge and exhibits anion selectivity. As the pH of the solution decreases from 11 to 3, more anions enter the positively charged nanoconfined structure, resulting in an increase of ionic current. This feature enables pH-induced gating characteristics and enhances the power density of osmotic power harvesters (Fig. 9(c)).

In summary, pH modulation dynamically adjusts the surface charge polarity and density within nanoconfined spaces, amplifying the ion selectivity of the EDL. This method enables precise control of ionic behavior, unlocking enhanced performance in iontronic applications like sensing, energy harvesting, and ion sieving.

### 4.6 Ion dynamics enhanced by concentration gradients

Concentration gradient-controlled ion dynamics leverages salinity gradients within nanoconfined spaces to drive ion diffusion, creating substantial driving forces that accelerate ion transport and enhance efficiency. This mechanism, coupled with EDL overlapped effects in nanoconfined spaces, enables rapid ionic flow through nanopores or nanochannels, producing high ionic currents. This approach significantly boosts performance in desalination, electrodialysis, water purification, and iontronic energy conversion and storage technologies.

For example, Jiang et al. reported an osmotic power generator based on a 3D Janus porous membrane with tunable surface charge density and porosity [128]. In this system, the Janus membrane is positioned between two reservoirs containing asymmetric salt concentrations (Fig. 10(a)). Driven by the concentration gradient, the membrane selectively filters ions with

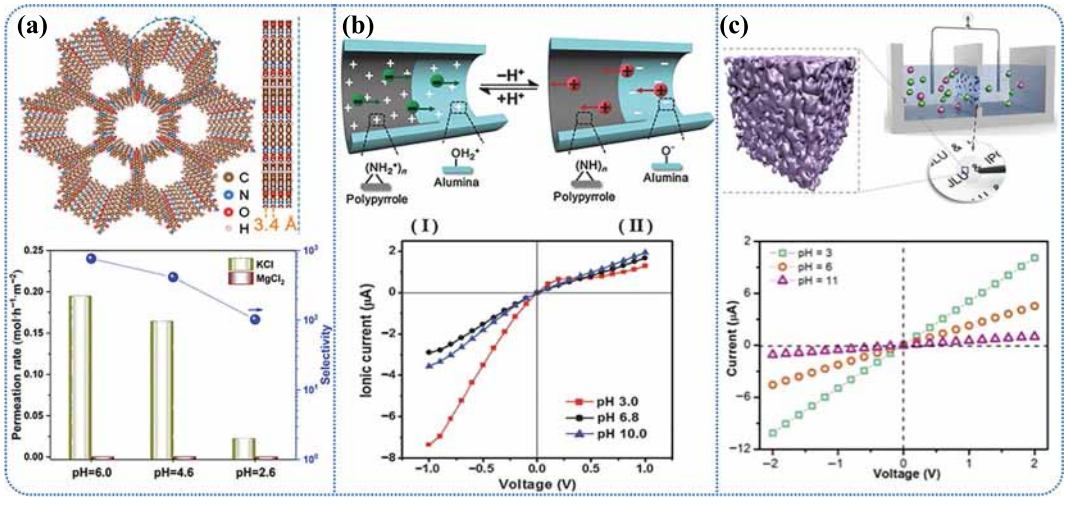


**Figure 9** Ion dynamics within nanoconfined spaces are controlled by pH. (a) The surface charge density of sub-2-nanometer COF membranes can be precisely controlled by pH to enhance osmotic energy conversion and ion sieving. Reproduced with permission from Ref. [125], © Wiley-VCH GmbH 2021. (b) Changes in surface charge, ion transport, and ionic current within the mixed nanoconfined structure ($PPy/Al_2O_3$) in response to variations in pH. Reproduced with permission from Ref. [126], © WILEY-VCH Verlag GmbH & Co. KGaA, Weinheim 2015. (c) Modulating the surface charge of a 3D polyphenylene sulfone membrane with pyridine side chains through pH leads to changes in ionic current. Reproduced with permission from Ref. [127], © Wiley-VCH GmbH 2020.

opposite charges while rejecting ions of the same polarity, generating a net ionic current. In a mixture of seawater and river water, the Janus membrane achieves a power density of 2.66 $W \cdot m^{-2}$, with an energy conversion efficiency of 35.7%. Increasing the salinity gradient enhances the output power density, reaching 5.10 $W \cdot m^{-2}$ at a 500-fold gradient, highlighting the potential for blue energy harvesting. In addition, hierarchically structured, anisotropic wood membranes also serve as efficient platforms for osmotic power harvesting. Natural wood possesses oriented nanochannels, which can be chemically modified *in situ* to introduce quaternary ammonium or carboxyl groups, imparting positive or negative charges to the channel surfaces. These ionized wood membranes function as ion exchange membranes, efficiently converting osmotic power (Fig. 10(b)) [129]. As the salinity gradient increases, these charged nanoconfined structures facilitate the selective transport of $Na^+$ and $Cl^-$ ions, generating higher ionic currents and enhanced osmotic power output. Under a 1000-fold concentration gradient, the ionic wood membrane-based osmotic power source can achieve a voltage of up to 184.4 mV and a current density of 286.3 $mA \cdot m^{-2}$. In addition, a standard silicon micromachining process was used to assemble dispersed negatively charged silica nanoparticles into $SiO_2$ crystals with face-centered cubic shape [43], thereby forming a $SiO_2$ nanoconfined structures (Fig. 10(c)). The $SiO_2$ membrane was subjected to different concentrations of KCl solution, and its Debye length ranges from 1 to 30 nm. The diffusion of $K^+$ ions in the nanoconfined spaces with concentration gradient and the overlapping EDL effect, generates an electric current. As the nanopore diameter decreases, the EDL overlapped effect is enhanced, which leads to a further increase in the conductivity and a power output of up to ~1.1 nW under 100 nm diameter. This precise modulation of ion dynamics in nanoconfined space provides an effective strategy for enhanced energy harvesting.

Concentration gradients drive ion diffusion and regulate transport within nanoconfined spaces by leveraging electrochemical potential differences, selective ion permeability, and ion-surface interactions. This mechanism is instrumental in advancing technologies for energy harvesting, storage, sensing, and gas separation.

## 5 Redefining electronics with complementary and distinct functionalities

Advancements in understanding EDL structures, combined with progress in nanotechnology and materials science, have propelled iontronics into diverse applications. Leveraging nanoconfined materials with overlapping EDL and enhanced ion dynamics, applications such as iontronic power sources, iontronic memristors, iontronic sensors, iontronic logic circuits, and iontronic filtering capacitors have overcome limitations of traditional electronics. These systems offer unique advantages, including environmental adaptability (e.g., tolerance to extreme temperatures, magnetic fields, and humidity), mechanical flexibility, self-healing properties, biosafety, superior performance, and reduced power consumption. Iontronics, rooted in nanoconfined spaces, is poised to bridge advanced electronics and biology, playing a transformative role in future human-machine interfaces and bio-robotics.

### 5.1 Iontronic power sources

Iontronic power sources are energy devices that generate and store energy through ionic-electronic coupling mechanisms. These systems leverage ion transport within nanoconfined spaces, where overlapping EDL enable efficient ion movement. When combined with external field modulation, these systems exhibit enhanced energy storage and harvesting capabilities. Iontronic power sources capture environmental energy via mechanisms such as osmosis, triboelectric effects, and photoelectric effects. Compared to conventional energy devices like batteries, supercapacitors, and fuel cells, iontronic power sources demonstrate superior biocompatibility, flexibility, cost-efficiency, environmental sustainability, and multifunctional integration. These advantages position iontronic power sources as promising solutions for wearable electronics, smart healthcare, and renewable energy technologies.

Harvesting atmospheric moisture to generate electricity offers a sustainable approach to iontronic energy collection. Qu et al. reported a moisture-enabled electric generator based on GO-functionalized paper for harvesting atmospheric moisture (Fig. 11(a)). This GO paper features an asymmetric surface charge

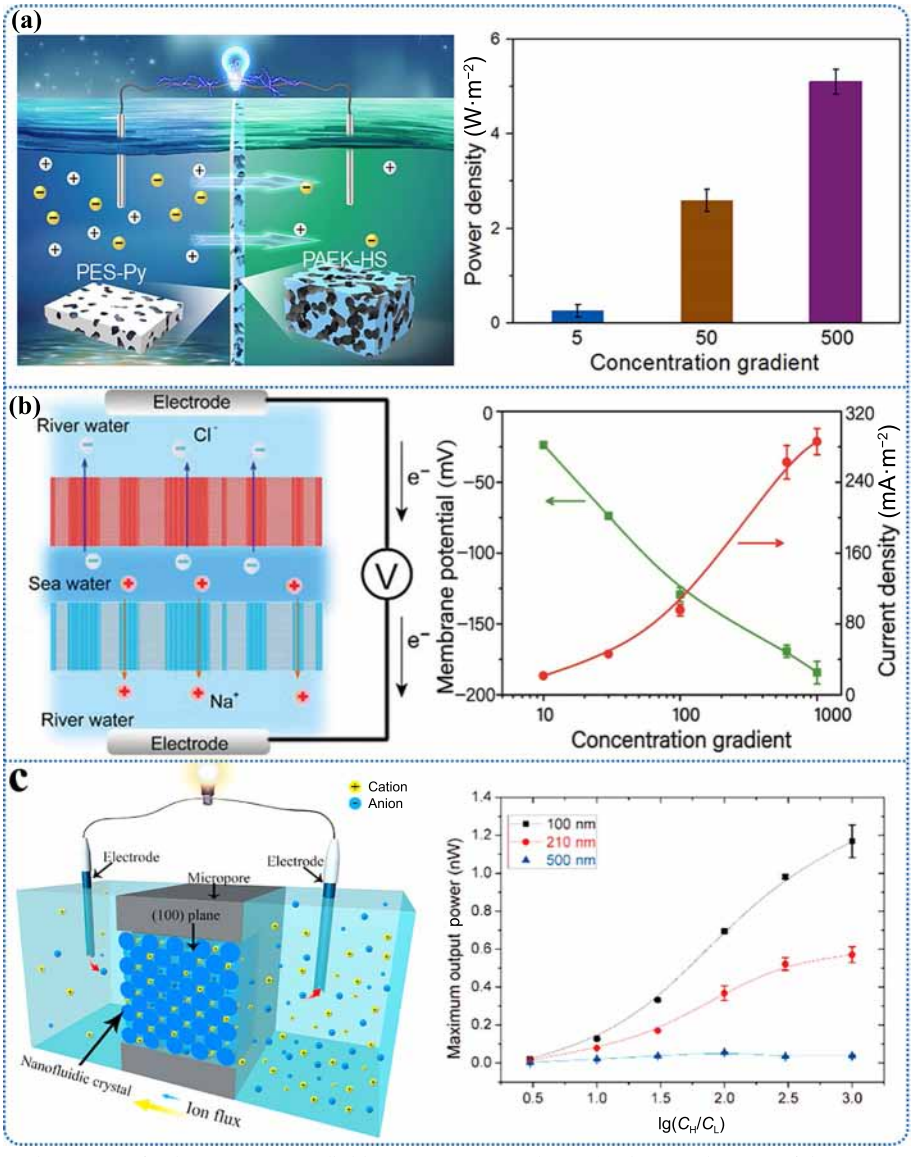


**Figure 10** Ion dynamics within nanoconfined spaces are controlled by concentration gradient. (a) Schematic depiction of the osmotic energy harvesting process under a concentration gradient based on the Janus porous membrane. Reproduced with permission from Ref. [128], © Zhu, X. et al. 2018. (b) Schematic diagram of an ionized wood membrane generating energy from the salinity gradient between river water and seawater. Reproduced with permission from Ref. [129], © WILEY-VCH Verlag GmbH & Co. KGaA, Weinheim 2019. (c) Schematic diagram of an osmotic energy harvesting device based on $SiO_2$ nanoconfined structures. Reproduced with permission from Ref. [43], © IOP Publishing Ltd. 2013.

density, which induces the formation of a $H^+$ gradient as its oxygen-containing functional groups absorb moisture. As moisture absorption increases, more $H^+$ ions are dissociated from the functionalized GO paper. These $H^+$ ions then move directionally within the nanoconfined space, generating a short-circuit current of 0.3 μA and an open-circuit voltage of 0.7 V [130]. Furthermore, the voltage output varies with changes in relative humidity. To further enhance the power output, a heterogeneous structure composed of gradient-reduced graphene oxide (grGO) and GO was employed (Fig. 11(b)). The gold electrode and silver electrode serve as the top and bottom electrodes of this heterostructure, respectively. In this configuration, $H^+$ ions move directionally through the moisture-absorbed grGO, generating power, while GO acts as a reservoir, replenishing $H^+$ carriers for grGO [131]. As a result, the moisture-enabled electric generator based on the grGO/GO heterogeneous structure achieves a voltage output of 1.5 V and a current of ~100 nA. This device, which efficiently captures atmospheric moisture to generate electrical energy, has garnered significant attention in recent studies.

Wei's group reported a solid-state iontronic power source based on osmotic effects coupled with redox reactions [14]. By printing GO and $K^+$-rich rGO ink onto flexible substrates, such as paper, with parallel Ag electrodes, they created GO nanoconfined channels with a height of ~7.7 Å. Humidity-driven $K^+$ transport through the negatively charged GO channels, facilitated by a chemical potential gradient and built-in electric field, generates electrical output. A single cell produces an open-circuit voltage of up to 1.2 V at 10% relative humidity (Fig. 11(c)), and connecting 175 cells in series on a paper strip achieves an ultra-high voltage of 192 V. Using a Peano space-filling curve design, the device delivers a short-circuit current of 170 μA and a power density of 2.5 $mW·cm^{-3}$, with an energy density comparable to lithium thin-film batteries at 0.41 $mWh·cm^{-3}$. The low-temperature performance of iontronic power sources is critical for portable electronics. Wei et al. developed a GO-based ultrathin iontronic

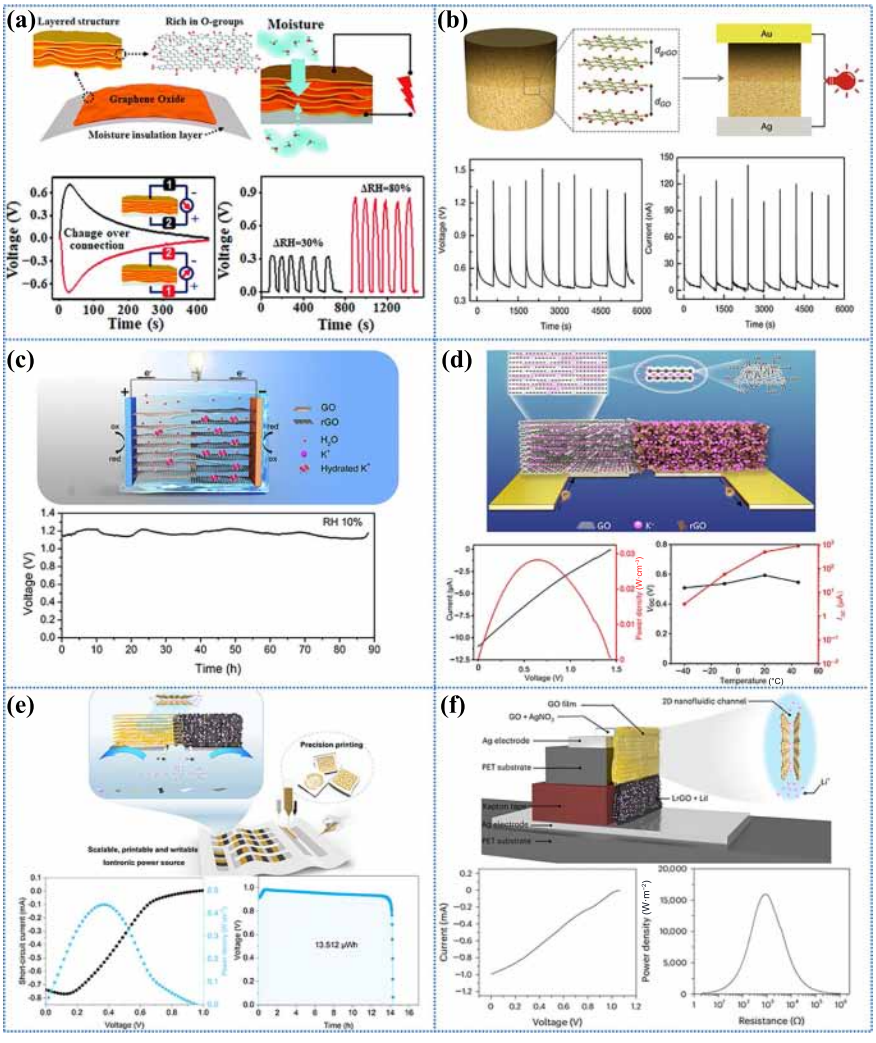


**Figure 11** Iontronic power sources based on regulation of ion dynamics by external field. (a) Iontronic power sources based on asymmetric functionalized graphene oxide paper. Reproduced with permission from Ref. [130], © The Royal Society of Chemistry 2018. (b) Iontronic power sources based on GO/rGO heterostructures. Reproduced with permission from Ref. [131], © Huang, Y. et al 2018. (c) $K^+$ ions, driven by moisture, migrate directionally under the influence of salinity gradients and redox reactions, thereby generating electrical energy. Reproduced with permission from Ref. [14], © Yang, L. et al 2021. (d) Iontronic power sources based on the migration of $Li^+$ within nanoconfined structures. Reproduced with permission from Ref. [15], © Wei, D. et al 2022. (e) Printable paper-based iontronic power sources. Reproduced with permission from Ref. [16], © Wiley-VCH GmbH 2023. (f) Iontronic power sources based on the transport of $Li^+$ in vertically nanoconfined structures. Reproduced with permission from Ref. [18], © Yang, F. et al 2024.

power source capable of generating 1.5 V and 11 μA (Fig. 11(d)) [15]. Integrated with triboelectric nanogenerators, this device forms a self-charging, flexible triboelectric-iontronic system. Graphene aerogels, prepared from GO/rGO with ion gel electrolytes, achieve an open-circuit voltage of 0.54 V and a short-circuit current of 57 μA at −10 °C. Remarkably, this device remains operational at temperatures as low as −40 °C, expanding its applicability to extreme environments. To tackle environmental challenges associated with heavy metals and toxic electrolytes, Wei's group also developed a paper-based iontronic power source. Driven by salinity gradients and interfacial redox reactions, $Li^+$ ions transport efficiently through negatively charged nanoconfined spaces [16]. The output voltage and current of the iontronic power source are ~1.0 V and ~700 μA, respectively, achieving a power density of 438.02 $mW{\cdot}cm^{-3}$. When discharged at a current of 1 μA, its energy density reaches up to 30.02 $mWh{\cdot}cm^{-3}$ (Fig. 11(e)). More importantly, this iontronic power source can be mass-produced on flexible substrates through a printable manner. The paper substrate's breathability, biocompatibility, and flexibility enable direct skin contact, providing continuous power for wearable devices. Additionally, the device supports efficient metal recovery through incineration, allowing electrodes to be separated from ashes and $Li^+$ ions to be reclaimed from liquid waste—an ideal method for recycling electrochemical energy storage systems. To further enhance power density, Wei et al. developed a vertically structured iontronic energy storage device using GO via ultrasonic spray coating. At 25 °C and 80% relative humidity, this device generates an open-circuit voltage of ~1 V and a short-circuit current of ~1 mA [18], achieving an exceptional power density of 15,900 $W{\cdot}m^{-2}$ (Fig. 11(f)). The vertical design facilitates rapid cation transport within nanoconfined spaces, reducing internal resistance. Voltage output scales nearly linearly with stacked devices. Unlike conventional batteries and supercapacitors, these iontronic power sources can be printed cost-effectively using commercial printing/spraying equipment.

### 5.2 Iontronic sensor

Iontronic sensors are a type of sensing device that operate based on ion transport and interaction within nanoconfined spaces or

ion-sensitive materials. These sensors detect specific ionic changes or variations in the ionic environment, which may be caused by factors such as concentration gradients, pH changes, or the presence of certain chemical species. Iontronic sensors typically rely on the ability to modulate ion movement or ion-electron interactions within a material in response to external stimuli. Iontronic sensors have distinct advantages over traditional electronic sensors, such as their potential for greater sensitivity, flexibility, and biocompatibility. They can be applied in fields like biomedical sensing (e.g., detecting specific biomarkers or pH levels in body fluids), environmental monitoring (e.g., water quality sensors), and chemical sensing (e.g., detecting ions in solutions). Their ability to operate in soft, flexible, and biocompatible materials also makes them ideal for wearable sensors and implantable devices.

For instance, Park et al. developed a nanosensor that combines nanoscale electrophoresis with nanopore sensing. This device achieves high-precision nucleotide identification by detecting transient longitudinal currents during molecule transit through nanopore columns of varying lengths (Fig. 12(a)) [132]. This method allows the differentiation of single molecules, vesicles, and particles based on distinct current signals. Jiang et al. engineered a molecular transport nano-gating system using nanoporous membranes functionalized with peptides. The peptides on the nanopore surface undergo reversible conformational changes between folded and random structures, triggered by oxygen and dithiothreitol (DTT) (Fig. 12(b)) [69]. This conformational switch enables precise control over molecular transport rates and dosages, facilitating targeted drug delivery. Similarly, Rant et al. utilized nitrilotriacetic acid (NTA)-modified metallized silicon nitride nanopores for protein sensing. His6-tagged proteins bind stably within the pore via NTA-His6 interactions (Fig. 12(c)) [133]. Real-time monitoring of current signals allows for the detection of protein binding and dissociation events, providing a powerful tool for proteomics. Iontronic systems are also effective for DNA detection. Elezgaray et al. created a DNA nanopore that undergoes conformational changes upon binding to a miR-21 miRNA analog (Fig. 12(d)) [134]. Fluorescent and electrical signal analysis confirmed the nanopore's ability to detect low concentrations of miRNA. Furthermore, micro-nanochannels fabricated via photolithography and wet etching can be functionalized with peptide nucleic acids (PNAs) (Fig. 12(e)) [135]. The high specificity of PNA-DNA interactions enables the detection of specific DNA sequences even at low concentrations. Chemically modified conical nanopores have also been developed for selective ion transport, mimicking biological ion-protein channels (Fig. 12(f)) [68]. These nanopores can precisely distinguish between $K^+$ and $Na^+$ ions, offering applications in clinical diagnostics and biosensing. In addition, nanoconfined iontronic sensors are also particularly useful for detecting toxic metal ions, which pose environmental and health hazards. By applying a bias voltage to a single nanopore in a high-salt solution, distinct electrical signals corresponding to different metal ions can be analyzed (Fig. 12(g)) [136]. This highly sensitive detection method holds promise for environmental monitoring and public health protection. Additionally, iontronic pressure sensors based on charge accumulation and dissipation in EDL interface have also been reported [137–139]. The iontronic pressure sensor's high-frequency resolution, negligible capacitive pressure hysteresis, and exceptional sensitivity endow it with a remarkable tactile perception capability, making it highly suitable for human-machine interaction applications [140–142].

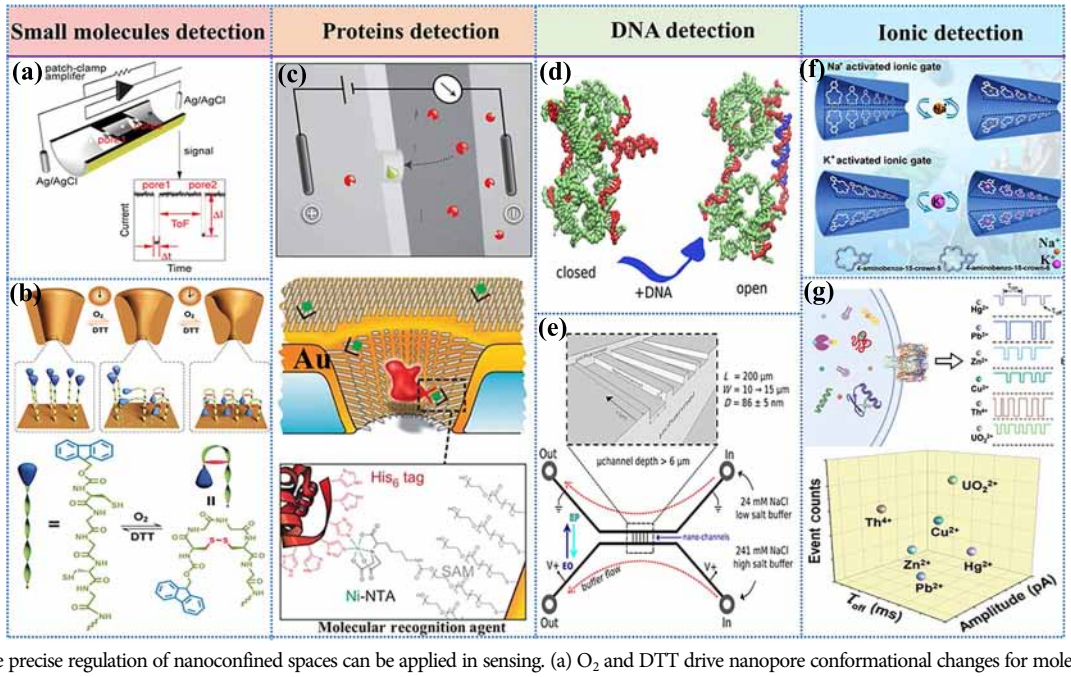


**Figure 12** The precise regulation of nanoconfined spaces can be applied in sensing. (a) $O_2$ and DTT drive nanopore conformational changes for molecular detection. Reproduced with permission from Ref. [132], © Wiley-VCH GmbH 2021. (b) $O_2$ and DTT drive nanopore conformational changes for molecular detection. Reproduced with permission from Ref. [69], © Wiley-VCH Verlag GmbH & Co. KGaA, Weinheim 2018. (c) Chemical modification of metallized nanopores for protein detection. Reproduced with permission from Ref. [133], © Macmillan Publishers Limited 2012. (d) Schematic diagram of the conformational change of DNA nanopores before and after binding with DNA analogs. Reproduced with permission from Ref. [134], © Wiley-VCH GmbH 2022. (e) Nanofluidic devices modified by peptide nucleic acids for DNA detection. Reproduced with permission from Ref. [135], © WILEY-VCH Verlag GmbH & Co. KGaA, Weinheim 2016. (f) Schematic diagram of simplified $Na^+$-activated and $K^+$-activated ionic gates. Reproduced with permission from Ref. [68], © American Chemical Society 2015. (g) A single nanopore sensor is used to differentiate between different metal ions by recording electrical signals. Reproduced with permission from Ref. [136], © Wiley-VCH GmbH 2020.

Finally, the precise control of ion transport and information storage within nanoconfined spaces makes iontronic sensors highly versatile. Unlike traditional sensors, which rely on electron flow, iontronic sensors utilize ions as charge carriers, offering flexible and tunable performance. The iontronic sensor based on nanoconfined structures effectively reduces noise and achieves sufficiently high signal-to-noise ratios in instantaneous ionic current signals, enabling precise detection of ions or molecules. This high-precision detection method provides a powerful tool for biosensing and environmental monitoring.

### 5.3 Iontronic logical components

Iontronic logic components represent an emerging field that leverages ions for logical operations and information processing. This technology encompasses iontronic memristors, diodes, transistors, and more. The key advantages of these ion-based components include low power consumption, high energy efficiency, and the ability to interface seamlessly with biological systems. These characteristics make iontronic logic components highly promising for applications in nonlinear computing, neuromorphic devices, and self-driven sensing systems.

#### *5.3.1 Iontronic memristors*

Iontronic memristors are a novel type of memory device that utilize ion transport and storage mechanisms. Unlike traditional electronic memory elements, such as resistive random-access memory (RRAM), iontronic memristors store and process information by regulating the migration and accumulation of ions within nanoconfined spaces, modulating conductivity and retaining the new state. A key feature of these memristors is their ability to enable reversible ion transport with low power consumption, offering high integration and multifunctionality. This makes them highly suitable for applications in neuromorphic computing, memory storage, logic operations, and signal processing. Thanks to the unique properties of ion transport, iontronic memristors can operate in flexible, biocompatible environments, with enhanced noise immunity and minimal energy consumption. As a result, they hold significant potential for emerging technologies, including wearable devices, brain-computer interfaces, and artificial intelligence.

For example, in biological systems, neurons act as dual-purpose units for processing and memory, transmitting signals via ions and neurotransmitters. Inspired by this energy-efficient architecture, Hou et al. integrated two charge-discharge nanofluidic memristors into a circuit modeled on the Hodgkin-Huxley framework (Fig. 13(a)) [6]. Experimental results showed that these 2D nanoconfined channels could generate voltage spike sequences analogous to biological neurons. This iontronic device, compatible with neuronal signals, operates with low power, making it a promising candidate for wearable and implantable iontronic devices, as well as neuron-computer interfaces. In addition, Bocquet et al. recently reported two types of nanoconfined channels that exhibit long-term memory and synapse-like ion dynamics. These two types of channels, composed of atomically smoothed $MoS_2$ sheets and activated carbon, which are separated by graphene nanoribbons or bilayer graphene sheets with etched nanogrooves, demonstrating memory effects in aqueous electrolytes (Fig. 13(b)) [23]. Furthermore, the conductive state of the iontronic memristor can be altered with variations by applying different magnitude and polarity of the voltages. These nanoconfined systems replicate synaptic plasticity by modulating ion accumulation and depletion. Fundamental learning algorithms, such as Hebbian learning, can be implemented in these simple nanoconfined structures. Leveraging nanoconfined effects to develop ion-based computational systems lays the groundwork for bio-inspired computing on aqueous electrochemical chips. Meanwhile, chemical synapses transmit signals via ion flux driven by neurotransmitters, offering inspiration for neuromorphic systems. For example, MOF nanoconfined channels modified with 2,3,6,7,10,11-hexaiminotriphenylene (Cu-HITP) and 2,3,6,7,10,11-hexahydroxytriphenylene (Cu-HHTP) produced nanofluidic synapses with opposite charges. These synapses exhibited enhanced or inhibited ion signaling behaviors regulated by glutamate (Glu). The introduction of glutamate oxidase (GluOx) catalyzed the conversion of Glu into electroactive $H_2O_2$, enabling selective chemical recognition by the oppositely charged synapses. Increasing Glu concentration resulted in distinct ion signaling behaviors (Fig. 13(c)) [70]. These nanofluidic synapses demonstrated plasticity and Hebbian learning, offering a blueprint for future applications in nanofluidic computing and brain-machine interfaces.

The precise control of ion transport and information storage within nanoconfined spaces imparts iontronic memristors with flexible and tunable performance, distinguishing them from traditional resistors that depend on electron transport. This unique capability positions iontronic memristors as promising candidates for next-generation computing and memory technologies.

#### *5.3.2 Iontronic diodes and transistors*

Iontronic logical components, including iontronic diodes and transistors, regulate ion movement within nanoconfined spaces or electrochemical environments to perform logical functions. An iontronic diode is a one-way ion transport device that permits ions to flow in one direction while blocking them in the opposite direction, similar to an electronic diode's electron flow. Iontronic diodes rely on asymmetric nanostructures or electrochemical gradients to induce ionic rectification. This rectification effect is influenced by external fields or applied voltage, which control ion migration through a membrane or nanostructured material. The ion flow asymmetry can be achieved by manipulating surface charge, nanoconfined spaces, or creating concentration gradients. These properties make iontronic diodes suitable for applications in ionic rectification, energy harvesting, and ion-based logic circuits. Iontronic transistors, on the other hand, use ions to modulate charge carriers within a device. Similar to electronic transistors, iontronic transistors rely on ion transport through a nanoconfined channel or electrochemical system. An ionic gate, typically made of a material that conducts ions (e.g., polymer electrolyte or gel), controls the ion flow between two electrodes or regions. By altering the ion concentration or distribution with a voltage, the gate modulates ionic current, much like how a conventional transistor controls electron flow. Iontronic transistors are integral to sensing, actuation, signal amplification, and bioelectronic devices, including brain-machine interfaces, where ionic currents naturally facilitate signaling.

Selective gated ion transport, akin to diodes and transistors in electronics, can be achieved by manipulating surface charge within nanoconfined spaces. Xia et al. developed a multivalent ion-responsive symmetric hourglass-shaped polycarbonate (PC) nanopore that exhibits high ionic rectification ratios (ICR) (Fig. 14(a)) [143]. In this device, two reservoirs are separated by a nanopore filled with KCl and potassium ferricyanide ($K_3Fe(CN)_6$).

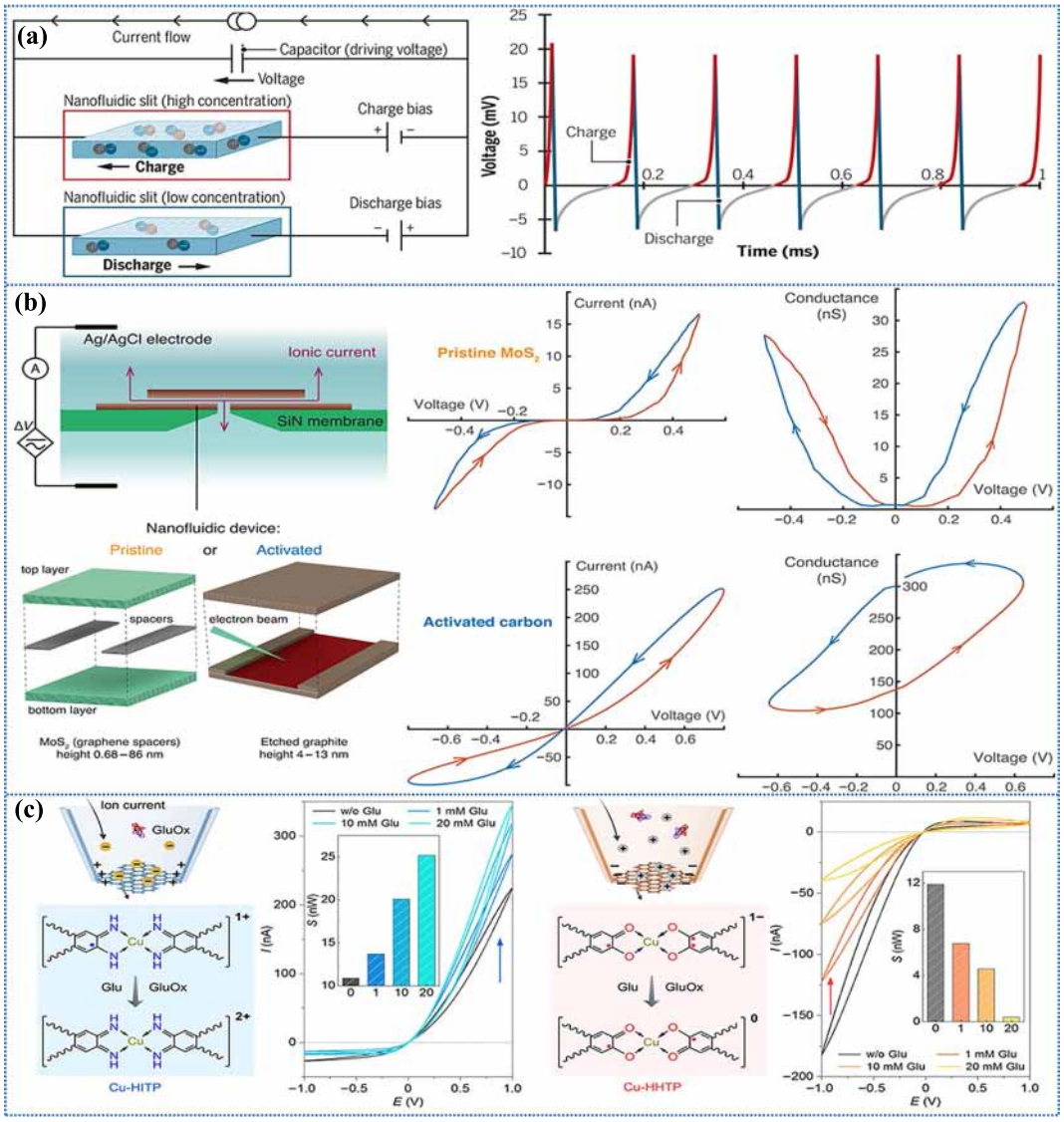


**Figure 13** Experimental study of the memristive effect in nanofluid devices. (a) Ionic memristors utilizing gel electrolytes. Reproduced with permission from Ref. [6], © Hou, Y. et al 2021. (b) Ionic memristors fabricated from molybdenum disulfide or activated carbon materials. Reproduced with permission from Ref. [23], © Robin, P. et al. 2023. (c) Glu-mediated MOF nanofluidic synapses. Reproduced with permission from Ref. [70], © American Chemical Society 2024.

Under negative voltage, $Fe^{3+}$ ions adsorb onto the nanopore surface, reversing the surface charge and resulting in an "OFF" state. This surface charge asymmetry leads to high ICR ratios, which increase with the concentration of multivalent ions. Additionally, pH-responsive ion gating can simulate the behavior of biological membranes. Block copolymers (BCP) form carboxyl groups in nanochannels upon UV irradiation, while AAO membranes, prepared via etching, exhibit hydroxyl-rich, uniform channels with diameters ranging from 10 to 200 nm (Fig. 14(b)) [144]. When a BCP film is placed on an AAO membrane, asymmetric organic-inorganic hybrid nanochannels are formed. By adjusting the solution pH between 3 and 11, the surface charge state of the nanochannels changes, enabling ion rectification behavior. Without the BCP film, this ion gating behavior is absent. Ion gating behavior can also be realized using graphene ion transistors (Fig. 14(c)) [113]. In the absence of voltage, hydrated ions are blocked due to their size exceeding the nanoconfined channel height, resulting in an "OFF" state. Applying a gate voltage alters the surface potential of the graphene layer, switching the system to an "ON" state by permitting ion permeation. Beyond unidirectional rectification, Reed et al. introduced a field-effect reconfigurable iontronic transistor controlled by asymmetric or double-split gates (Fig. 14(d)) [27]. Sequential surface treatments with 3-glycidoxypropyltrimethoxysilane and ethanolamine reduce the native surface charge of $SiO_2$ nanoconfined channels. By applying a voltage of +1 or −1 V to asymmetric gate electrodes, bidirectional ion rectification can be achieved. This dual-gate system enables precise control over ion transport direction and rectification degree.

In contrast to ion diodes, which depend on stimulus-responsive properties, reconfigurable iontronic transistors provide independent, digitally programmable control over ion and molecule transport. These transistors hold significant promise as key components for the large-scale integration of ion logic circuits.

### 5.4 Iontronic filter capacitors

The capacitor's ability to filter out ripples in a circuit can be attributed to its charge and discharge behavior, which forms the essential basis of its filtering function. When the capacitor charges, it can store more charge, causing the voltage across the capacitor

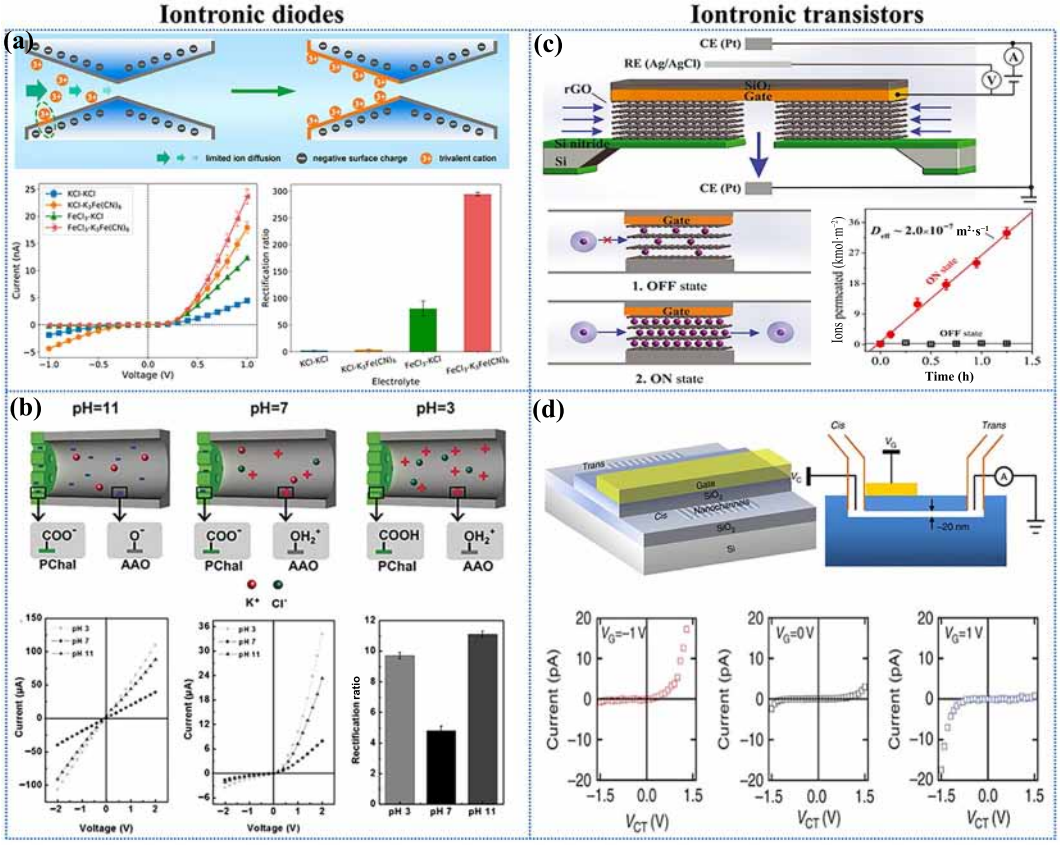


**Figure 14** Rectification effect of iontronic diodes and transistors achieved through external field. (a) Iontronic diodes realized based on symmetric hourglass-shaped PC nanopores. Reproduced with permission from Ref. [143], © American Chemical Society 2019. (b) Rectification of iontronic diodes achieved through pH-controlled surface charge of nanoconfined structures. Reproduced with permission from Ref. [144], © Wiley-VCH Verlag GmbH & Co. KGaA, Weinheim 2016. (c) Schematic diagram of a voltage-gated device based on a graphene nanoconfined channel. Reproduced with permission from Ref. [113], © Xue, Y. et al. 2021. (d) Gate-controlled behavior of iontronic transistors realized by controlling the gate voltage of a graphene nanoconfined structures. Reproduced with permission from Ref. [27], © Macmillan Publishers Limited 2011.

to gradually rise, which helps smooth voltage fluctuations and reduce noise. When the input voltage drops, the capacitor can release the stored charge, which helps compensate for the instantaneous voltage drop, thereby maintaining a stable output voltage. Iontronic filter capacitors represent a new class of capacitors that exploit the synergistic interaction between ionic and electronic charge transport to deliver enhanced filtering performance, particularly in high-frequency applications.

Efficient ripple filtering in iontronic capacitors depends on the rapid transport of ions within nanoconfined channels at the electrode-electrolyte interface, enabling superior signal processing and noise reduction. For instance, Miller et al. synthesized vertically oriented graphene nanosheets directly on heated nickel (Ni) substrates using chemical vapor deposition to serve as electrodes for iontronic filter capacitors (Fig. 15(a)) [33]. These electrodes feature EDL-enhanced nanoconfined spaces and high-density active sites, which significantly reduce ion and electron transport resistance. This results in improved performance at high frequencies, with the iontronic filter capacitor showing a much better impedance phase angle at high frequencies (at 120 Hz, phase angle = –82°) compared to commercial electrolytic capacitors. This makes it a promising alternative to traditional aluminum electrolytic capacitors for filtering applications. In a similar vein, Shi et al. developed an ultrahigh-rate iontronic capacitor based on nitrogen-doped holey graphene (NHG) thin films (Fig. 15(b)). The hierarchical holey nanoconfined structure of the NHG films facilitates rapid $H^+$ ion transport, leading to enhanced ion movement within the electrodes. These NHG-based iontronic filter capacitors exhibit high areal (478 μF·cm$^{-2}$) and volumetric (1.2 F·cm$^{-3}$) capacitance, ultrafast ion transport, and excellent frequency response (at 120 Hz, phase angle = –81.2°) [145], making them well-suited for AC line filtering applications. Iontronic capacitors can also be fabricated using electrochemically rGO films with fewer defects as electrodes (Fig. 15(c)) [146]. These electrodes feature a 3D interconnected porous nanoconfined structure that enhances ion dynamics within the electrolyte, maintaining excellent filtering performance even under high-frequency scanning (at 120 Hz, phase angle = –81.2°). To further improve frequency response, PEDOT : poly(styrenesulfonate) (PEDOT:PSS) is used as a binder to connect rGO nanosheets, forming a highly conductive network for iontronic capacitors (Fig. 15(d)) [147]. This conductive network enables rapid ion transport within the nanoconfined space, resulting in a high ionic current and an ultrahigh frequency response (at 120 Hz, phase angle = –81.41°) with outstanding filtering performance. Additionally, a multi-layer carbon tube (MLCT) framework serves as a high-performance electrode (Fig. 15(e)). By controlling the number of carbon tube layers, the density of nanoconfined channels is increased, achieving a specific capacitance of 3.08 mF·cm$^{-2}$ and a phase angle of –80.1° at 120 Hz. The high density, orientation, and integrity of the carbon tube array facilitate the rapid transport and distribution of $H^+$ ions, imparting excellent capacitance and frequency response. As a result, ripple signals are effectively filtered, yielding a smooth output [73]. To

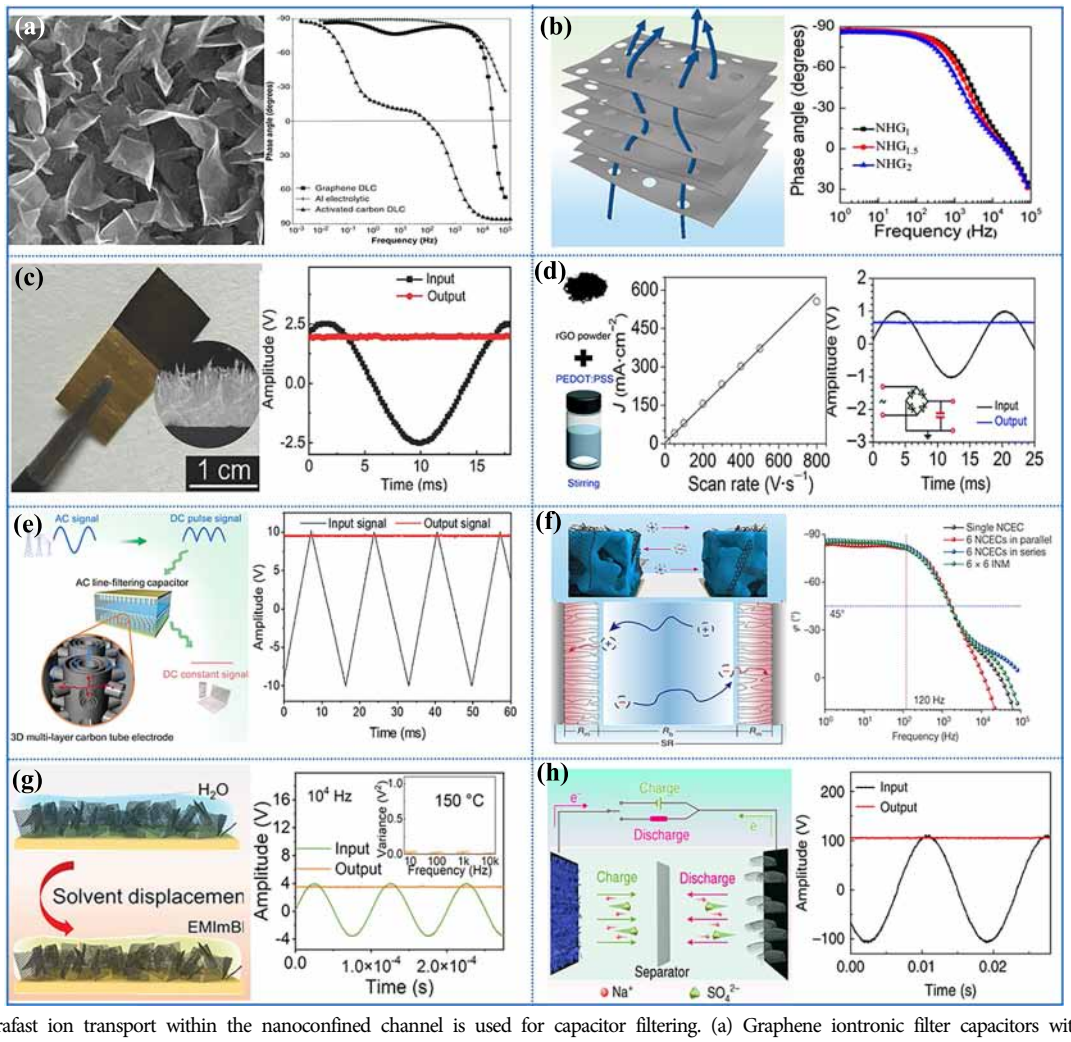


**Figure 15** Ultrafast ion transport within the nanoconfined channel is used for capacitor filtering. (a) Graphene iontronic filter capacitors with line-filtering performance. Reproduced with permission from Ref. [33], © Miller, J. et al. 2010. (b) Ultrafast iontronic filter capacitors based on nitrogen-doped porous graphene films for line filtering. Reproduced with permission from Ref. [145], © American Chemical Society 2016. (c) Iontronic filter capacitors based on electrochemically reduced graphene oxide for line filtering. Reproduced with permission from Ref. [146], © WILEY-VCH Verlag GmbH & Co. KGaA, Weinheim 2017. (d) Iontronic filter capacitors based on highly conductive graphene films for line filtering. Reproduced with permission from Ref. [147], © The Royal Society of Chemistry 2018. (e) Iontronic filtering capacitors based on a multilayer carbon tube framework. Reproduced with permission from Ref. [73], © The Royal Society of Chemistry 2018. (f) High-performance filtering capacitor enabled by the electric field enhancement strategy. Reproduced with permission from Ref. [72], © Hu, Y. et al 2023. (g) Ultrafast iontronic filter capacitors based on graphene ion gel. Reproduced with permission from Ref. [148], © Wiley-VCH GmbH 2022. (h) Electrochemical reduction of graphene oxide as the iontronic filter capacitor's negative electrode to achieve high-frequency filtering. Reproduced with permission from Ref. [149], © Wu, M. et al. 2019.

further enhance filtering performance, Qu et al. proposed an electric field enhancement strategy to promote ion migration within both electrode materials and the electrolyte. Using femtosecond lasers, channels are precisely cut into the electrode (Fig. 15(f)), increasing the interaction between electrode channels and ions. This facilitates rapid ion transport, resulting in a low series resistance of 39 mΩ·cm$^{-2}$ at 120 Hz [72]. The lightweight design of these capacitors enables easy integration into circuit boards for AC filtering applications. As integrated circuits advance, filtering capacitors face increasing demands for high-power and high-temperature performance (e.g., >100 °C in monitoring electronics). A vertically oriented graphene ion gel electrode has recently been developed for ultrafast electrochemical capacitors (Fig. 15(g)) [148]. The vertical graphene nanochannels enable rapid ion transport, achieving a phase angle of –80° at 120 Hz. Additionally, the ion gel allows stable filtering of arbitrary AC waveforms at temperatures up to 150 °C. To meet the needs of multi-scenario applications, Qu et al. also reported a filtering capacitor capable of operating at 200 V without compromising performance. This capacitor utilizes acid-treated PEDOT films and electrochemically reduced graphene oxide (ErGO) sheets as the positive and negative electrodes, respectively (Fig. 15(h)) [149]. Both materials offer high conductivity and porous structures, facilitating rapid ion and electron transport with excellent EDL capacitance. At 120 Hz, the capacitor achieves a phase angle of –82° and effectively filters ripple at 200 V, demonstrating its suitability for various high-performance applications.

Iontronic filter capacitors leverage ultrafast ion transport within nanoconfined channels, introducing a novel mechanism distinct from traditional capacitors that depend solely on electronic charge movement. By utilizing ion migration within electrolytes or nanostructured materials, these capacitors achieve enhanced capacitance and superior signal filtering performance. The ionic-electronic coupling inherent in iontronic capacitors enables effective high-frequency signal filtering, significantly reducing ripple and noise while ensuring energy efficiency. Their unique

tenability, achieved by modifying electrolyte composition and electrode materials, further allows for precise optimization tailored to advanced applications, such as signal processing in Central Processing Units (CPUs). This adaptability, combined with exceptional high-frequency response, reduced energy losses, and improved operational stability, positions iontronic filter capacitors as a transformative alternative to conventional capacitors, paving the way for advancements in power management, signal processing, and flexible electronic systems.

## 6 Conclusion and perspectives

Nanoconfined iontronics, inspired by biological ion channels, is redefining electronics by offering complementary and distinct functionalities that traditional electronics cannot achieve. By precisely regulating ion transport within nanoscale structures, iontronics introduces a paradigm shift in how we understand and harness ion dynamics. This review highlights the significant advances in understanding the EDL in nanoconfined spaces, tracing the evolution from foundational EDL models to the development of 0D to 3D nanomaterials. These materials, with their enhanced ion dynamics driven by overlapping EDL effects, form the cornerstone of next-generation iontronic devices. The integration of external physical fields, such as electric fields, light, heat, and pressure, along with chemical fields like pH variations and concentration gradients, has allowed for increasingly precise control over ion transport, broadening the applications of iontronics. These innovations have driven advancements in energy conversion, sensing, logic circuits, and high-frequency filtering. Unlike conventional electronic systems, iontronic devices offer unparalleled advantages, such as biocompatibility, flexibility, environmental adaptability, low power consumption, and multifunctionality. With their ability to interface with biological systems and function under diverse conditions, iontronic devices are poised to revolutionize fields like wearable technology, brain-machine interfaces, neuromorphic computing, and renewable energy harvesting, offering new capabilities beyond the reach of traditional electronics.

Despite significant advancements, nanoconfined iontronics faces several challenges that must be overcome to enable broader application and commercialization. The scalability and cost-effectiveness of fabricating nanoscale iontronic devices remain key obstacles due to the complexity of current manufacturing processes. The development of efficient, one-step synthesis methods is crucial for large-scale production. Additionally, enhancing the flexibility and stretchability of nanoconfined materials is essential to meet the increasing demand for wearable and implantable devices. A deeper understanding of anomalous ion transport mechanisms in nanoconfined spaces is also needed. Integrating in situ characterization techniques with advanced simulations, such as finite element analysis, molecular dynamics, and density functional theory, can provide valuable insights into these processes. Moreover, ensuring long-term stability and durability under extreme conditions, including high temperatures, varying pH, and mechanical stress, is critical for practical applications. The integration of multiple iontronic logic units into complex systems remains a challenge, requiring scalable architectures for integrated circuits to advance ion-based information processing and neuromorphic computing. Lastly, addressing the environmental impact and sustainability of iontronic devices is imperative, particularly for applications in water desalination, pollutant detection, and renewable energy. In perspective, unlocking the full potential of nanoconfined iontronics will position it as a transformative technology that redefines traditional electronics. By enabling the precise control of ion transport in nanoconfined spaces, iontronics can complement and enhance the functionalities of conventional electronic systems, offering distinct advantages such as biocompatibility, flexibility, and environmental adaptability. As this field matures, iontronics is poised to revolutionize industries such as energy, sensing, computing, and bioelectronics, forging a new path that bridges the gap between traditional electronics and biological systems. Ultimately, nanoconfined iontronics represents a promising frontier that will extend the capabilities of electronics, offering complementary and distinct functionalities that are currently beyond the reach of conventional electronic technologies.

## Acknowledgements

This work was supported by the National Natural Science Foundation of China (No. 22479016).

## Declaration of conflicting interests

The authors declare no conflicting interests regarding the content of this article.

## Data availability

All data needed to support the conclusions in the paper are presented in the manuscript and/or the Supplementary Materials. Additional data related to this paper may be requested from the corresponding author upon request.

## References

[1] Chun, H.; Chung, T. D. Iontronics. *Annu. Rev. Anal. Chem.* **2015**, *8*, 441–462.

[2] Peng, P. G.; Qian, H.; Liu, J. J.; Wang, Z. L.; Wei, D. Bioinspired ionic control for energy and information flow. *Int. J. Smart Nano Mater.* **2024**, *15*, 198–221.

[3] Goldhaber-Gordon, D.; Montemerlo, M. S.; Love, J. C.; Opiteck, G. J.; Ellenbogen, J. C. Overview of nanoelectronic devices. *Proc. IEEE* **1997**, *85*, 521–540.

[4] Arbring Sjöström, T.; Berggren, M.; Gabrielsson, E. O.; Janson, P.; Poxson, D. J.; Seitanidou, M.; Simon, D. T. A decade of iontronic delivery devices. *Adv. Mater. Technol.* **2018**, *3*, 1700360.

[5] Bisri, S. Z.; Shimizu, S.; Nakano, M.; Iwasa, Y. Endeavor of iontronics: From fundamentals to applications of ion-controlled electronics. *Adv. Mater.* **2017**, *29*, 1607054.

[6] Hou, Y. Q.; Hou, X. Bioinspired nanofluidic iontronics. *Science* **2021**, *373*, 628–629.

[7] Bocquet, L.; Charlaix, E. Nanofluidics, from bulk to interfaces. *Chem. Soc. Rev.* **2010**, *39*, 1073–1095.

[8] Kim, B.; Heo, J.; Kwon, H. J.; Cho, S. J.; Han, J.; Kim, S. J.; Lim, G. Tunable ionic transport for a triangular nanochannel in a polymeric nanofluidic system. *ACS Nano* **2013**, *7*, 740–747.

[9] Devine, M. J.; Kittler, J. T. Mitochondria at the neuronal presynapse in health and disease. *Nat. Rev. Neurosci.* **2018**, *19*, 63–80.

[10] Huang, J.; Pan, X. J.; Yan, N. E. Structural biology and molecular pharmacology of voltage-gated ion channels. *Nat. Rev. Mol. Cell Biol.* **2024**, *25*, 904–925.

[11] Yu, X. M.; Salter, M. W. Gain control of NMDA-receptor currents by intracellular sodium. *Nature* **1998**, *396*, 469–474.

[12] Steinberg-Yfrach, G.; Rigaud, J. L.; Durantini, E. N.; Moore, A. L.; Gust, D.; Moore, T. A. Light-driven production of ATP catalysed by $F_0F_1$-ATP synthase in an artificial photosynthetic membrane. *Nature* **1998**, *392*, 479–482.

[13] Wei, D. Writable electrochemical energy source based on graphene oxide. *Sci. Rep.* **2015**, *5*, 15173.

[14] Yang, L.; Yang, F. Y.; Liu, X.; Li, K.; Zhou, Y. N.; Wang, Y. J.; Yu, T. H.; Zhong, M. J.; Xu, X. B.; Zhang, L. J. et al. A moisture-enabled fully printable power source inspired by electric eels. *Proc. Natl. Acad. Sci. USA* **2021**, *118*, e2023164118.

[15] Wei, D.; Yang, F. Y.; Jiang, Z. H.; Wang, Z. L. Flexible iontronics based on 2D nanofluidic material. *Nat. Commun.* **2022**, *13*, 4965.

[16] Peng, P. G.; Yang, F. Y.; Wang, Z. L.; Wei, D. Integratable paper-based iontronic power source for all-in-one disposable electronics. *Adv. Energy Mater.* **2023**, *13*, 2302360.

[17] Peng, P. G.; Yang, F. Y.; Li, X.; Li, S. X.; Wang, Z. L.; Wei, D. High-power iontronics enabled by nanoconfined ion dynamics. *Cell Rep. Phys. Sci.* **2024**, *5*, 101824.

[18] Yang, F. Y.; Peng, P. G.; Yan, Z. Y.; Fan, H. Z.; Li, X.; Li, S. X.; Liu, H. F.; Ren, T. L., Zhou, Y. G.; Wang, Z. L. et al. Vertical iontronic energy storage based on osmotic effects and electrode redox reactions. *Nat. Energy* **2024**, *9*, 263–271.

[19] Li, C. C.; Cheng, J. X.; He, Y. F.; He, X. N.; Xu, Z. Y.; Ge, Q.; Yang, C. H. Polyelectrolyte elastomer-based ionotronic sensors with multi-mode sensing capabilities via multi-material 3D printing. *Nat. Commun.* **2023**, *14*, 4853.

[20] Cheng, Y.; Zhan, Y. F.; Guan, F. Y.; Shi, J. L.; Wang, J. X.; Sun, Y.; Zubair, M.; Yu, C. J.; Guo, C. F. Displacement-pressure biparametrically regulated softness sensory system for intraocular pressure monitoring. *Natl. Sci. Rev.* **2024**, *11*, nwae050.

[21] Zhang, Y.; Zhou, X. M.; Zhang, N.; Zhu, J. Q.; Bai, N. N.; Hou, X. Y.; Sun, T.; Li, G.; Zhao, L. Y.; Chen, Y. C. et al. Ultrafast piezocapacitive soft pressure sensors with over 10 kHz bandwidth via bonded microstructured interfaces. *Nat. Commun.* **2024**, *15*, 3048.

[22] Wang, D. C.; Kvetny, M.; Liu, J.; Brown, W.; Li, Y.; Wang, G. L. Transmembrane potential across single conical nanopores and resulting memristive and memcapacitive ion transport. *J. Am. Chem. Soc.* **2012**, *134*, 3651–3654.

[23] Robin, P.; Emmerich, T.; Ismail, A.; Niguès, A.; You, Y.; Nam, G. H.; Keerthi, A.; Siria, A.; Geim, A. K.; Radha, B. et al. Long-term memory and synapse-like dynamics in two-dimensional nanofluidic channels. *Science* **2023**, *379*, 161–167.

[24] Xu, G. H.; Zhang, M. L.; Mei, T. T.; Liu, W. C.; Wang, L.; Xiao, K. Nanofluidic ionic memristors. *ACS Nano* **2024**, *18*, 19423–19442.

[25] Yu, L. J.; Li, X. P.; Luo, C. Y.; Lei, Z. K.; Wang, Y. L.; Hou, Y. Q.; Wang, M.; Hou, X. Bioinspired nanofluidic iontronics for brain-like computing. *Nano Res.* **2024**, *17*, 503–514.

[26] Hao, J. R.; Wu, R.; Zhou, J. L.; Zhou, Y. H.; Jiang, L. Regulation of bioinspired ion diodes: From fundamental study to blue energy harvesting. *Nano Today* **2022**, *46*, 101593.

[27] Guan, W. H.; Fan, R.; Reed, M. A. Field- effect reconfigurable nanofluidic ionic diodes. *Nat. Commun.* **2011**, *2*, 506.

[28] Huang, X. D.; Kong, X. Y.; Wen, L. P.; Jiang, L. Bioinspired ionic diodes: From unipolar to bipolar. *Adv. Funct. Mater.* **2018**, *28*, 1801079.

[29] Mei, T. T.; Liu, W. C.; Sun, F. S.; Chen, Y. X.; Xu, G. H.; Huang, Z. J.; Jiang, Y. S.; Wang, S. Y.; Chen, L.; Liu, J. J. et al. Bio-inspired two-dimensional nanofluidic ionic transistor for neuromorphic signal processing. *Angew. Chem., Int. Ed.* **2024**, *63*, e202401477.

[30] Mei, T. T.; Liu, W. C.; Xu, G. H.; Chen, Y. X.; Wu, M. H.; Wang, L.; Xiao, K. Ionic transistors. *ACS Nano* **2024**, *18*, 4624–4650.

[31] Karnik, R.; Fan, R.; Yue, M.; Li, D. Y.; Yang, P. D.; Majumdar, A. Electrostatic control of ions and molecules in nanofluidic transistors. *Nano Lett.* **2005**, *5*, 943–948.

[32] Fan, R.; Yue, M.; Karnik, R.; Majumdar, A.; Yang, P. D. Polarity switching and transient responses in single nanotube nanofluidic transistors. *Phys. Rev. Lett.* **2005**, *95*, 086607.

[33] Miller, J. R.; Outlaw, R. A.; Holloway, B. C. Graphene double-layer capacitor with AC line-filtering performance. *Science* **2010**, *329*, 1637–1639.

[34] Wu, Z. S.; Liu, Z. Y.; Parvez, K.; Feng, X. L.; Müllen, K. Ultrathin printable graphene supercapacitors with AC line-filtering performance. *Adv. Mater.* **2015**, *27*, 3669–3675.

[35] Zhang, M.; Zhou, Q. Q.; Chen, J.; Yu, X. W.; Huang, L.; Li, Y. R.; Li, C.; Shi, G. Q. An ultrahigh-rate electrochemical capacitor based on solution-processed highly conductive PEDOT:PSS films for AC line-filtering. *Energy Environ. Sci.* **2016**, *9*, 2005–2010.

[36] Xu, S. C.; Shen, C.; Peng, Z. S.; Wu, J. D.; Chen, Z.; Zhang, X. Y.; Ji, N. N.; Jian, M. Q.; Wu, M. M.; Gao, X. et al. Direct growth of vertical graphene on fiber electrodes and its application in alternating current line-filtering capacitors. *ACS Nano* **2024**, *18*, 24154–24161.

[37] Zhao, M. M.; Qin, Y. C.; Wang, X. Y.; Wang, L. X.; Jin, Q.; Song, M. R.; Wang, X. P.; Qu, L. T. PEDOT:PSS/Ketjenblack holey nanosheets with ultrahigh areal capacitance for kHz AC line-filtering micro-supercapacitors. *Adv. Funct. Mater.* **2024**, *34*, 2313495.

[38] Sun, J. Y.; Zhao, X. H.; Illeperuma, W. R. K.; Chaudhuri, O.; Oh, K. H.; Mooney, D. J.; Vlassak, J. J.; Suo, Z. G. Highly stretchable and tough hydrogels. *Nature* **2012**, *489*, 133–136.

[39] Freed, L. E.; Engelmayr, G. C. Jr.; Borenstein, J. T.; Moutos, F. T.; Guilak, F. Advanced material strategies for tissue engineering scaffolds. *Adv. Mater.* **2009**, *21*, 3410–3418.

[40] Zhang, J. R.; Liu, W. C.; Dai, J. Q.; Xiao, K. Nanoionics from biological to artificial systems: An alternative beyond nanoelectronics. *Adv. Sci.* **2022**, *9*, 2200534.

[41] Robin, P.; Bocquet, L. Nanofluidics at the crossroads. *J. Chem. Phys.* **2023**, *158*, 160901.

[42] Lei, Y. H.; Wang, W.; Wu, W. G.; Li, Z. H. Nanofluidic diode in a suspended nanoparticle crystal. *Appl. Phys. Lett.* **2010**, *96*, 263102.

[43] Ouyang, W.; Wang, W.; Zhang, H. X.; Wu, W. G.; Li, Z. H. Nanofluidic crystal: A facile, high-efficiency and high-power-density scaling up scheme for energy harvesting based on nanofluidic reverse electrodialysis. *Nanotechnology* **2013**, *24*, 345401.

[44] Heiranian, M.; Farimani, A. B.; Aluru, N. R. Water desalination with a single-layer $MoS_2$ nanopore. *Nat. Commun.* **2015**, *6*, 8616.

[45] Siria, A.; Poncharal, P.; Biance, A. L.; Fulcrand, R.; Blase, X.; Purcell, S. T.; Bocquet, L. Giant osmotic energy conversion measured in a single transmembrane boron nitride nanotube. *Nature* **2013**, *494*, 455–458.

[46] Cui, G. D.; Xu, Z.; Li, H.; Zhang, S. C.; Xu, L. P.; Siria, A.; Ma, M. Enhanced osmotic transport in individual double-walled carbon nanotube. *Nat. Commun.* **2023**, *14*, 2295.

[47] Chen, C.; Liu, D.; He, L.; Qin, S.; Wang, J. M.; Razal, J. M.; Kotov, N. A.; Lei, W. W. Bio-inspired nanocomposite membranes for osmotic energy harvesting. *Joule* **2020**, *4*, 247–261.

[48] Zhang, Z.; Yang, S.; Zhang, P. P.; Zhang, J.; Chen, G. B.; Feng, X. L. Mechanically strong MXene/Kevlar nanofiber composite membranes as high-performance nanofluidic osmotic power generators. *Nat. Commun.* **2019**, *10*, 2920.

[49] Liu, G. P.; Jin, W. Q.; Xu, N. P. Two-dimensional-material membranes: A new family of high-performance separation membranes. *Angew. Chem., Int. Ed.* **2016**, *55*, 13384–13397.

[50] Zhang, Z.; He, L.; Zhu, C. C.; Qian, Y. C.; Wen, L. P.; Jiang, L. Improved osmotic energy conversion in heterogeneous membrane boosted by three-dimensional hydrogel interface. *Nat. Commun.* **2020**, *11*, 875.

[51] Hu, Y. X.; Wei, J.; Liang, Y.; Zhang, H. C.; Zhang, X. W.; Shen, W.; Wang, H. T. Zeolitic imidazolate framework/graphene oxide hybrid nanosheets as seeds for the growth of ultrathin molecular sieving membranes. *Angew. Chem., Int. Ed.* **2016**, *55*, 2048–2052.

[52] Chen, W. P.; Wang, Q.; Chen, J. J.; Zhang, Q. R.; Zhao, X. L.; Qian, Y. C.; Zhu, C. C.; Yang, L. S.; Zhao, Y. Y.; Kong, X. Y. et al. Improved ion transport and high energy conversion through hydrogel membrane with 3D interconnected nanopores. *Nano Lett.* **2020**, *20*, 5705–5713.

[53] Jiang, Y. S.; Liu, W. C.; Wang, T.; Wu, Y. T.; Mei, T. T.; Wang,

L.; Xu, G. H.; Wang, Y. D.; Liu, N. N.; Xiao, K. A nanofluidic chemoelectrical generator with enhanced energy harvesting by ion-electron Coulomb drag. *Nat. Commun.* **2024**, *15*, 8582.

[54] Yeom, J.; Choe, A.; Lee, J.; Kim, J.; Kim, J.; Oh, S. H.; Park, C.; Na, S.; Shin, Y. E.; Lee, Y. et al. Photosensitive ion channels in layered MXene membranes modified with plasmonic gold nanostars and cellulose nanofibers. *Nat. Commun.* **2023**, *14*, 359.

[55] Gao, Y. F.; Zhang, Z. J.; Zhao, X.; Wang, Y.; Sun, L. X.; Cao, S. X.; Lei, Y.; Li, B. H.; Zhou, D.; Kang, F. Y. "Island-bridge"-structured nanofluidic membranes for high-performance aqueous energy conversion and storage. *Energy Mater. Devices* **2024**, *2*, 9370041.

[56] Chen, K. X.; Yao, L. N.; Su, B. Bionic thermoelectric response with nanochannels. *J. Am. Chem. Soc.* **2019**, *141*, 8608–8615.

[57] Yin, S. J.; Li, J. G.; Lai, Z. Z.; Meng, Q. W.; Xian, W. P.; Dai, Z. F.; Wang, S.; Zhang, L.; Xiong, Y. B.; Ma, S. Q. et al. Giant gateable thermoelectric conversion by tuning the ion linkage interactions in covalent organic framework membranes. *Nat. Commun.* **2024**, *15*, 8137.

[58] Guo, W.; Cheng, C.; Wu, Y. Z.; Jiang, Y. N.; Gao, J.; Li, D.; Jiang, L. Bio-inspired two-dimensional nanofluidic generators based on a layered graphene hydrogel membrane. *Adv. Mater.* **2013**, *25*, 6064–6068.

[59] He, Y. F.; Cheng, Y.; Yang, C. H.; Guo, C. F. Creep-free polyelectrolyte elastomer for drift-free iontronic sensing. *Nat. Mater.* **2024**, *23*, 1107–1114.

[60] Liu, Z. G.; Cai, M. K.; Hong, S. D.; Shi, J. L.; Xie, S.; Liu, C.; Du, H. F.; Morin, J. D.; Li, G.; Wang, L. et al. Data- driven inverse design of flexible pressure sensors. *Proc. Natl. Acad. Sci. USA.* **2024**, *121*, e2320222121.

[61] Mei, T. T.; Zhang, H. J.; Xiao, K. Bioinspired artificial ion pumps. *ACS Nano* **2022**, *16*, 13323–13338.

[62] Awati, A.; Yang, R.; Shi, T.; Zhou, S.; Zhang, X.; Zeng, H.; Lv, Y. K.; Liang, K.; Xie, L.; Zhu, D. Z. et al. Interfacial super-assembly of vacancy engineered ultrathin-nanosheets toward nanochannels for smart ion transport and salinity gradient power conversion. *Angew. Chem., Int. Ed.* **2024**, *63*, e202407491.

[63] Xin, W. W.; Zhang, Z.; Huang, X. D.; Hu, Y. H.; Zhou, T.; Zhu, C. C.; Kong, X. Y.; Jiang, L.; Wen, L. P. High-performance silk-based hybrid membranes employed for osmotic energy conversion. *Nat. Commun.* **2019**, *10*, 3876.

[64] Zhang, Z. K.; Shen, W. H.; Lin, L. X.; Wang, M.; Li, N.; Zheng, Z. F.; Liu, F.; Cao, L. X. Vertically transported graphene oxide for high-performance osmotic energy conversion. *Adv. Sci.* **2020**, *7*, 2000286.

[65] Peng, P. G.; Shen, P. H.; Qian, H.; Liu, J. J.; Lu, H.; Jiao, Y. Y.; Yang, F. Y.; Liu, H. F.; Ren, T. L.; Wang, Z. L. et al. Photochemical iontronics with multitype ionic signal transmission at single pixel for self-driven color and tridimensional vision. *Device*, in press, DOI: 10.1016/j.device.2024.100574.

[66] Liu, Y. H.; Li, Z. H.; Wang, L. Y.; Yang, X. J.; Yang, Y.; Li, X. S.; Jiang, Y.; Gao, Y.; Lü, W. Surface functional modification for boosting power density of hydrovoltaic devices. *Adv. Funct. Mater.* **2024**, *34*, 2312666.

[67] Liu, Y. H.; Li, Z. H.; Yang, X. J.; Yang, Y.; Li, X. S.; Jiang, Y.; Gao, Y.; Wang, L. Y.; Lü, W. Multifunctional power generators beyond moisture limitation. *Adv. Funct. Mater.* **2024**, *34*, 2407204.

[68] Liu, Q.; Xiao, K.; Wen, L. P.; Lu, H.; Liu, Y. H.; Kong, X. Y.; Xie, G. H.; Zhang, Z.; Bo, Z. S.; Jiang, L. Engineered ionic gates for ion conduction based on sodium and potassium activated nanochannels. *J. Am. Chem. Soc.* **2015**, *137*, 11976–11983.

[69] Xiao, K.; Wu, K.; Chen, L.; Kong, X. Y.; Zhang, Y. Q.; Wen, L. P.; Jiang, L. Biomimetic peptide-gated nanoporous membrane for on-demand molecule transport. *Angew. Chem., Int. Ed.* **2018**, *57*, 151–155.

[70] Yu, S. Y.; Hu, J.; Li, Z.; Xu, Y. T.; Yuan, C.; Jiang, D. C.; Zhao, W. W. Metal- organic framework nanofluidic synapse. *J. Am. Chem. Soc.* **2024**, *146*, 27022–27029.

[71] Li, M. Q.; Wang, C. F.; Liu, Z. J.; Song, Y. X.; Li, D. Q. Ionic diode based on an asymmetric-shaped carbon black nanoparticle membrane. *Adv. Funct. Mater.* **2021**, *31*, 2104341.

[72] Hu, Y. J.; Wu, M. M.; Chi, F. Y.; Lai, G. B.; Li, P. Y.; He, W. Y.; Lu, B.; Weng, C. X.; Lin, J. G.; Chen, F. G. et al. Ultralow-resistance electrochemical capacitor for integrable line filtering. *Nature* **2023**, *624*, 74–79.

[73] Chen, G.; Han, F. M.; Lin, D.; Zhang, S. P.; Pan, Q. J.; Shao, C.; Wang, Z. M.; Zhu, X. G.; Meng, G. W.; Wei, B. Q. Three-dimensional multi-layer carbon tube electrodes for AC line-filtering capacitors. *Joule* **2024**, *8*, 1080–1091.

[74] Zhang, X.; Qu, Z. G.; Wang, Q.; Iqbal, M. Geometry design and mechanism analysis of artificial nanoroughness for enhanced osmotic energy conversion. *Energy Convers. Manage.* **2022**, *273*, 116373.

[75] Li, X.; Wang, Z. L.; Wei, D. Scavenging energy and information through dynamically regulating the electrical double layer. *Adv. Funct. Mater.* **2024**, *34*, 2405520.

[76] Bocquet, L. Concluding remarks: Iontronics, from fundamentals to ion-controlled devices-random access memories. *Faraday Discuss.* **2023**, *246*, 618–622.

[77] Helmholtz, H. Ueber einige Gesetze der Vertheilung elektrischer Ströme in körperlichen Leitern mit Anwendung auf die thierisch-elektrischen Versuche. *Ann. Phys.* **1853**, *165*, 211–233.

[78] Gouy, M. Sur la constitution de la charge électrique à la surface d' un électrolyte. *J. Phys. Theor. Appl.* **1910**, *9*, 457–468.

[79] Stern, O. Zur theorie der elektrolytischen doppelschicht. *Z. Elektrochem. Angew. Phys. Chem.* **1924**, *30*, 508–516.

[80] Grahame, D. C. The electrical double layer and the theory of electrocapillarity. *Chem. Rev.* **1947**, *41*, 441–501.

[81] Bockris, J. O. M.; Devanathan, M. A. V.; Müller, K. On the structure of charged interfaces. *Proc. Roy. Soc. A: Math. Phys. Eng. Sci.* **1963**, *274*, 55–79.

[82] Vacic, A.; Criscione, J. M.; Rajan, N. K.; Stern, E.; Fahmy, T. M.; Reed, M. A. Determination of molecular configuration by Debye length modulation. *J. Am. Chem. Soc.* **2011**, *133*, 13886–13889.

[83] Stern, E.; Wagner, R.; Sigworth, F. J.; Breaker, R.; Fahmy, T. M.; Reed, M. A. Importance of the debye screening length on nanowire field effect transistor sensors. *Nano Lett.* **2007**, *7*, 3405–3409.

[84] Wang, M.; Hou, Y. Q.; Yu, L. J.; Hou, X. Anomalies of ionic/molecular transport in nano and sub-nano confinement. *Nano Lett.* **2020**, *20*, 6937–6946.

[85] Feng, J. D.; Liu, K.; Graf, M.; Dumcenco, D.; Kis, A.; Di Ventra, M.; Radenovic, A. Observation of ionic Coulomb blockade in nanopores. *Nat. Mater.* **2016**, *15*, 850–855.

[86] Kondrat, S.; Wu, P.; Qiao, R.; Kornyshev, A. A. Accelerating charging dynamics in subnanometre pores. *Nat. Mater.* **2014**, *13*, 387–393.

[87] Zhang, S. G.; Zhang, J. H.; Zhang, Y.; Deng, Y. Q. Nanoconfined ionic liquids. *Chem. Rev.* **2017**, *117*, 6755–6833.

[88] Kim, S.; Choi, S.; Lee, H. G.; Jin, D. N.; Kim, G.; Kim, T.; Lee, J. S.; Shim, W. Neuromorphic van der Waals crystals for substantial energy generation. *Nat. Commun.* **2021**, *12*, 47.

[89] Kim, S. J.; Wang, Y. C.; Lee, J. H.; Jang, H.; Han, J. Concentration polarization and nonlinear electrokinetic flow near a nanofluidic channel. *Phys. Rev. Lett.* **2007**, *99*, 044501.

[90] Kim, S. J.; Ko, S. H.; Kang, K. H.; Han, J. Direct seawater desalination by ion concentration polarization. *Nat. Nanotechnol.* **2010**, *5*, 297–301.

[91] Pu, Q. S.; Yun, J.; Temkin, H.; Liu, S. R. Ion-enrichment and ion-depletion effect of nanochannel structures. *Nano Lett.* **2004**, *4*, 1099–1103.

[92] Gopinadhan, K.; Hu, S.; Esfandiar, A.; Lozada-Hidalgo, M.; Wang, F. C.; Yang, Q.; Tyurnina, A. V.; Keerthi, A.; Radha, B.; Geim, A. K. Complete steric exclusion of ions and proton transport through confined monolayer water. *Science* **2019**, *363*, 145–148.

[93] Yu, J. Y.; Marchesi D'Alvise, T.; Harley, I.; Krysztofik, A.; Lieberwirth, I.; Pula, P.; Majewski, P. W.; Graczykowski, B.;

Hunger, J.; Landfester, K. et al. Ion and molecular sieving with ultrathin polydopamine nanomembranes. *Adv. Mater.* **2024**, *36*, 2401137.

[94] Sun, Q.; Song, Z. Y.; Du, J. C.; Yao, A. Y.; Liu, L. H.; He, W.; Hassan, S. U.; Guan, J.; Liu, J. T. Covalent organic framework membranes with regulated orientation for monovalent cation sieving. *ACS Nano* **2024**, *18*, 27065–27076.

[95] Zhao, W. D.; Wang, B. J.; Wang, W. Biochemical sensing by nanofluidic crystal in a confined space. *Lab. Chip* **2016**, *16*, 2050–2058.

[96] Shang, X. M.; Xie, G. H.; Kong, X. Y.; Zhang, Z.; Zhang, Y. Q.; Tian, W.; Wen, L. P.; Jiang, L. An artificial $CO_2$-driven ionic gate inspired by olfactory sensory neurons in mosquitoes. *Adv. Mater.* **2017**, *29*, 1603884.

[97] Choi, E.; Wang, C.; Chang, G. T.; Park, J. High current ionic diode using homogeneously charged asymmetric nanochannel network membrane. *Nano Lett.* **2016**, *16*, 2189–2197.

[98] Lang, C.; Li, W. F.; Dong, Z. Y.; Zhang, X.; Yang, F. H.; Yang, B.; Deng, X. L.; Zhang, C. Y.; Xu, J. Y.; Liu, J. Q. Biomimetic transmembrane channels with high stability and transporting efficiency from helically folded macromolecules. *Angew. Chem., Int. Ed.* **2016**, *55*, 9723–9727.

[99] Wang, J.; Zhang, Z. J.; Zhu, J. N.; Tian, M. T.; Zheng, S. C.; Wang, F. D.; Wang, X. D.; Wang, L. Ion sieving by a two-dimensional $Ti_3C_2T_x$ alginate lamellar membrane with stable interlayer spacing. *Nat. Commun.* **2020**, *11*, 3540.

[100] Wang, Y.; Lian, T. T.; Tarakina, N. V.; Yuan, J. Y.; Antonietti, M. Lamellar carbon nitride membrane for enhanced ion sieving and water desalination. *Nat. Commun.* **2022**, *13*, 7339.

[101] Yang, L. X.; Cao, L. N. Y.; Li, S. X.; Peng, P. G.; Qian, H.; Amaratunga, G.; Yang, F. Y.; Wang, Z. L.; Wei, D. MOFs/MXene nano-hierarchical porous structures for efficient ion dynamics. *Nano Energy* **2024**, *129*, 110076.

[102] Xiao, S. Y.; Meng, K. X.; Xie, Q.; Zhai, L. X.; Xu, Z. P.; Wang, H.; Duan, C. H. Edge- enhanced ultrafast water evaporation from graphene nanopores. *Cell Rep. Phys. Sci.* **2022**, *3*, 100900.

[103] Cohen-Tanugi, D.; Grossman, J. C. Water desalination across nanoporous graphene. *Nano Lett.* **2012**, *12*, 3602–3608.

[104] Wang, H. Y.; Jian, G. Q.; Yan, S.; DeLisio, J. B.; Huang, C.; Zachariah, M. R. Electrospray formation of gelled nano-aluminum microspheres with superior reactivity. *ACS Appl. Mater. Interfaces* **2013**, *5*, 6797–6801.

[105] Xue, G. B.; Xu, Y.; Ding, T. P.; Li, J.; Yin, J.; Fei, W. W.; Cao, Y. Z.; Yu, J.; Yuan, L. Y.; Gong, L. et al. Water-evaporation-induced electricity with nanostructured carbon materials. *Nat. Nanotechnol.* **2017**, *12*, 317–321.

[106] Graf, M.; Lihter, M.; Altus, D.; Marion, S.; Radenovic, A. Transverse detection of DNA using a $MoS_2$ nanopore. *Nano Lett.* **2019**, *19*, 9075–9083.

[107] Hoenig, E.; Han, Y.; Xu, K. L.; Li, J. Y.; Wang, M. Z.; Liu, C. *In situ* generation of (sub) nanometer pores in $MoS_2$ membranes for ion-selective transport. *Nat. Commun.* **2024**, *15*, 7911.

[108] Zhu, J. N.; Wang, L.; Wang, J.; Wang, F. D.; Tian, M. T.; Zheng, S. C.; Shao, N.; Wang, L. L.; He, M. L. Precisely tunable ion sieving with an $Al_{13}$–$Ti_3C_2T_x$ lamellar membrane by controlling interlayer spacing. *ACS Nano* **2020**, *14*, 15306–15316.

[109] Politano, A.; Argurio, P.; Di Profio, G.; Sanna, V.; Cupolillo, A.; Chakraborty, S.; Arafat, H. A.; Curcio, E. Photothermal membrane distillation for seawater desalination. *Adv. Mater.* **2017**, *29*, 1603504.

[110] Tan, J. J.; Hu, J. Y.; Ren, J. X.; Peng, J. F.; Liu, C.; Song, Y. Q.; Zhang, Y. Fast response speed of mechanically exfoliated $MoS_2$ modified by PbS in detecting $NO_2$. *Chin. Chem. Lett.* **2020**, *31*, 2103–2108.

[111] Plett, T. S.; Cai, W. J.; Le Thai, M.; Vlassiouk, I. V.; Penner, R. M.; Siwy, Z. S. Solid- state ionic diodes demonstrated in conical nanopores. *J. Phys. Chem. C* **2017**, *121*, 6170–6176.

[112] Qian, H.; Peng, P. G.; Fan, H. Z.; Yang, Z.; Yang, L. X.; Zhou, Y. G.; Tan, D.; Yang, F. Y.; Willatzen, M.; Amaratunga, G. et al. Horizontal transport in $Ti_3C_2T_x$ MXene for highly efficient osmotic energy conversion from saline-alkali environments. *Angew. Chem., Int. Ed.* **2024**, *63*, e202414984.

[113] Xue, Y. H.; Xia, Y.; Yang, S.; Alsaid, Y.; Fong, K. Y.; Wang, Y.; Zhang, X. Atomic- scale ion transistor with ultrahigh diffusivity. *Science* **2021**, *372*, 501–503.

[114] Ouyang, Y. W.; Li, X.; Li, S. X.; Wang, Z. L.; Wei, D. Ionic rectification by dynamic regulation of the electric double layer at the hydrogel interface. *ACS Appl. Mater. Interfaces* **2024**, *16*, 18236–18244.

[115] Pérez-Mitta, G.; Marmisollé, W. A.; Trautmann, C.; Toimil-Molares, M. E.; Azzaroni, O. An all-plastic field-effect nanofluidic diode gated by a conducting polymer layer. *Adv. Mater.* **2017**, *29*, 1700972.

[116] Wang, Y. Q.; Zhang, H. C.; Kang, Y.; Zhu, Y. L.; Simon, G. P.; Wang, H. T. Voltage-gated ion transport in two-dimensional sub-1 nm nanofluidic channels. *ACS Nano* **2019**, *13*, 11793–11799.

[117] Liu, P.; Zhou, T.; Teng, Y. F.; Fu, L.; Hu, Y. H.; Lin, X. B.; Kong, X. Y.; Jiang, L.; Wen, L. P. Light-induced heat driving active ion transport based on 2D MXene nanofluids for enhancing osmotic energy conversion. *CCS Chem.* **2021**, *3*, 1325–1335.

[118] Yang, J. L.; Hu, X. Y.; Kong, X.; Jia, P.; Ji, D. Y.; Quan, D.; Wang, L. L.; Wen, Q.; Lu, D. N.; Wu, J. Z. et al. Photo-induced ultrafast active ion transport through graphene oxide membranes. *Nat. Commun.* **2019**, *10*, 1171.

[119] Ouyang, Y. W.; Li, X.; Li, S. X.; Peng, P. G.; Yang, F. Y.; Wang, Z. L.; Wei, D. Opto- iontronic coupling in triboelectric nanogenerator. *Nano Energy* **2023**, *116*, 108796.

[120] Wang, Q. C.; Wu, Y. D.; Zhu, C. C.; Hu, Y. H.; Fu, L.; Qian, Y. C.; Zhang, Z. H.; Li, T.; Li, X.; Kong, X. Y. et al. Efficient solar-osmotic power generation from bioinspired anti-fouling 2D $WS_2$ composite membranes. *Angew. Chem., Int. Ed.* **2023**, *62*, e202302938.

[121] Zhang, P. C.; Chen, S. F.; Zhu, C. J.; Hou, L. X.; Xian, W. P.; Zuo, X. H.; Zhang, Q. H.; Zhang, L.; Ma, S. Q.; Sun, Q. Covalent organic framework nanofluidic membrane as a platform for highly sensitive bionic thermosensation. *Nat. Commun.* **2021**, *12*, 1844.

[122] Ren, H. Y.; Tang, M.; Guan, B. L.; Wang, K. X.; Yang, J. W.; Wang, F. F.; Wang, M. Z.; Shan, J. Y.; Chen, Z. L.; Wei, D. et al. Hierarchical graphene foam for efficient omnidirectional solar-thermal energy conversion. *Adv. Mater.* **2017**, *29*, 1702590.

[123] Yi, F.; Ren, H. Y.; Dai, K. R.; Wang, X. F.; Han, Y. Z.; Wang, K. X.; Li, K.; Guan, B. L.; Wang, J.; Tang, M. et al. Solar thermal-driven capacitance enhancement of supercapacitors. *Energy Environ. Sci.* **2018**, *11*, 2016–2024.

[124] Chun, K. Y.; Son, Y. J.; Han, C. S. Highly sensitive and patchable pressure sensors mimicking ion-channel-engaged sensory organs. *ACS Nano* **2016**, *10*, 4550–4558.

[125] Sheng, F. M.; Wu, B.; Li, X. Y.; Xu, T. T.; Shehzad, M. A.; Wang, X. X.; Ge, L.; Wang, H. T.; Xu, T. W. Efficient ion sieving in covalent organic framework membranes with sub-2-nanometer channels. *Adv. Mater.* **2021**, *33*, 2104404.

[126] Zhang, Q. Q.; Liu, Z. Y.; Wang, K. F.; Zhai, J. Organic/inorganic hybrid nanochannels based on polypyrrole-embedded alumina nanopore arrays: pH- and light-modulated ion transport. *Adv. Funct. Mater.* **2015**, *25*, 2091–2098.

[127] Zhu, X. B.; Zhong, J. D.; Hao, J. R.; Wang, Y. Z.; Zhou, J. J.; Liao, J. W.; Dong, Y. J.; Pang, J. H.; Zhang, H. B.; Wang, Z. Z. et al. Polymeric nano-blue-energy generator based on anion-selective ionomers with 3D pores and pH-driving gating. *Adv. Energy Mater.* **2020**, *10*, 2001552.

[128] Zhu, X. B.; Hao, J. R.; Bao, B.; Zhou, Y. H.; Zhang, H. B.; Pang, J. H.; Jiang, Z. H.; Jiang, L. Unique ion rectification in hypersaline environment: A high-performance and sustainable power generator system. *Sci. Adv.* **2018**, *4*, eaau1665.

[129] Wu, Q. Y.; Wang, C. W.; Wang, R. L.; Chen, C. J.; Gao, J. L.; Dai, J. Q.; Liu, D. P.; Lin, Z. W.; Hu, L. B. Salinity- gradient power generation with ionized wood membranes. *Adv. Energy Mater.* **2020**, *10*, 1902590.

[130] Liang, Y.; Zhao, F.; Cheng, Z. H.; Deng, Y. X.; Xiao, Y. K.;

Cheng, H. H.; Zhang, P. P.; Huang, Y. X.; Shao, H. B.; Qu, L. T. Electric power generation via asymmetric moisturizing of graphene oxide for flexible, printable and portable electronics. *Energy Environ. Sci.* **2018**, *11*, 1730–1735.

[131] Huang, Y. X.; Cheng, H. H.; Yang, C.; Zhang, P. P.; Liao, Q. H.; Yao, H. Z.; Shi, G. Q.; Qu, L. T. Interface-mediated hygroelectric generator with an output voltage approaching 1.5 volts. *Nat. Commun.* **2018**, *9*, 4166.

[132] Choi, J.; Jia, Z.; Riahipour, R.; McKinney, C. J.; Amarasekara, C. A.; Weerakoon-Ratnayake, K. M.; Soper, S. A.; Park, S. Label-free identification of single mononucleotides by nanoscale electrophoresis. *Small* **2021**, *17*, 2102567.

[133] Wei, R. S.; Gatterdam, V.; Wieneke, R.; Tampé, R.; Rant, U. Stochastic sensing of proteins with receptor-modified solid-state nanopores. *Nat. Nanotechnol.* **2012**, *7*, 257–263.

[134] Yang, L. Y.; Cullin, C.; Elezgaray, J. Detection of short DNA sequences with DNA nanopores. *ChemPhysChem* **2022**, *23*, e202200021.

[135] Startsev, M. A.; Ostrowski, M.; Goldys, E. M.; Inglis, D. W. A mobility shift assay for DNA detection using nanochannel gradient electrophoresis. *Electrophoresis* **2017**, *38*, 335–341.

[136] Roozbahani, G. M.; Chen, X. H.; Zhang, Y. W.; Wang, L.; Guan, X. Y. Nanopore detection of metal ions: Current status and future directions. *Small Methods* **2020**, *4*, 2000266.

[137] Li, R. Y.; Si, Y.; Zhu, Z. J.; Guo, Y. J.; Zhang, Y. J.; Pan, N.; Sun, G.; Pan, T. R. Supercapacitive iontronic nanofabric sensing. *Adv. Mater.* **2017**, *29*, 1700253.

[138] Qiu, Z. G.; Wan, Y. B.; Zhou, W. H.; Yang, J. Y.; Yang, J. L.; Huang, J.; Zhang, J. M.; Liu, Q. X.; Huang, S. Y.; Bai, N. N. et al. Ionic skin with biomimetic dielectric layer templated from *Calathea zebrine* leaf. *Adv. Funct. Mater.* **2018**, *28*, 1802343.

[139] Zhu, Z. J.; Li, R. Y.; Pan, T. R. Imperceptible epidermal-iontronic interface for wearable sensing. *Adv. Mater.* **2018**, *30*, 1705122.

[140] Bai, N. N.; Wang, L.; Wang, Q.; Deng, J.; Wang, Y.; Lu, P.; Huang, J.; Li, G.; Zhang, Y.; Yang, J. L. et al. Graded intrafillable architecture-based iontronic pressure sensor with ultra-broad-range high sensitivity. *Nat. Commun.* **2020**, *11*, 209.

[141] Chang, Y.; Wang, L.; Li, R. Y.; Zhang, Z. C.; Wang, Q.; Yang, J. L.; Guo, C. F.; Pan, T. R. First decade of interfacial iontronic sensing: From droplet sensors to artificial skins. *Adv. Mater.* **2021**, *33*, 2003464.

[142] Lu, P.; Wang, L.; Zhu, P.; Huang, J.; Wang, Y. J.; Bai, N. N.; Wang, Y.; Li, G.; Yang, J. L.; Xie, K. W. et al. Iontronic pressure sensor with high sensitivity and linear response over a wide pressure range based on soft micropillared electrodes. *Sci. Bull.* **2021**, *66*, 1091–1100.

[143] Li, Z. Q.; Wang, Y.; Wu, Z. Q.; Wu, M. Y.; Xia, X. H. Bioinspired multivalent ion responsive nanopore with ultrahigh ion current rectification. *J. Phys. Chem. C* **2019**, *123*, 13687–13692.

[144] Sui, X.; Zhang, Z. Y.; Zhang, Z.; Wang, Z. W.; Li, C.; Yuan, H.; Gao, L. C.; Wen, L. P.; Fan, X.; Yang, L. J. et al. Biomimetic nanofluidic diode composed of dual amphoteric channels maintains rectification direction over a wide pH range. *Angew. Chem., Int. Ed.* **2016**, *55*, 13056–13060.

[145] Zhou, Q. Q.; Zhang, M.; Chen, J.; Hong, J. D.; Shi, G. Q. Nitrogen-doped holey graphene film-based ultrafast electrochemical capacitors. *ACS Appl. Mater. Interfaces* **2016**, *8*, 20741–20747.

[146] Chi, F. Y.; Li, C.; Zhou, Q. Q.; Zhang, M.; Chen, J.; Yu, X. W.; Shi, G. Q. Graphene-based organic electrochemical capacitors for AC line filtering. *Adv. Energy Mater.* **2017**, *7*, 1700591.

[147] Zhang, M.; Yu, X. W.; Ma, H. Y.; Du, W. C.; Qu, L. T.; Li, C.; Shi, G. Q. Robust graphene composite films for multifunctional electrochemical capacitors with an ultrawide range of areal mass loading toward high-rate frequency response and ultrahigh specific capacitance. *Energy Environ. Sci.* **2018**, *11*, 559–565.

[148] Chi, F. Y.; Hu, Y. J.; He, W. Y.; Weng, C. X.; Cheng, H. H.; Li, C.; Qu, L. T. Graphene ionogel ultra-fast filter supercapacitor with 4 V workable window and 150 °C operable temperature. *Small* **2022**, *18*, 2200916.

[149] Wu, M. M.; Chi, F. Y.; Geng, H. Y.; Ma, H. Y.; Zhang, M.; Gao, T. T.; Li, C.; Qu, L. T. Arbitrary waveform AC line filtering applicable to hundreds of volts based on aqueous electrochemical capacitors. *Nat. Commun.* **2019**, *10*, 2855.

**Yanhui Liu** achieved the B.S. degree from the Linyi University in 2021 and the M.S. degree from Changchun University of Technology in 2024. Now, he continues pursuing the Ph.D. degree at Beijing Institute of Nanoenergy and Nanosystems, Chinese Academy of Sciences. His research interest is solid-liquid contact electrification.

**Puguang Peng** achieved the B.S. and M.S. degrees from the Xiangtan University in 2019 and 2022, respectively. He continues pursuing Ph.D. degree in Beijing Institute of Nanoenergy and Nanosystems, Chinese Academy of Sciences. He focuses on the transformation of ions and electrons, with the applications in iontronics, energy technology and intelligent sensing systems.

**Han Qian** is a master's student at University of Chinese Academy of Sciences. He achieved the B.S. degree from Henan University of Science and Technology in 2023. He focuses on the transformation of ions and electrons, with the applicatons in iontronics and osmotic energy harvesting.

**Zhong Lin Wang** received his Ph.D. from Arizona State University in physics. He now is the Hightower Chair in Materials Science and Engineering, Regents' Professor, Engineering Distinguished Professor and Director, Center for Nanostructure Characterization, at Georgia Tech. Dr. Wang has made original and innovative contributions to the synthesis, discovery, characterization and understanding of fundamental physical properties of oxide nanobelts and nanowires, as well as applications of nanowires in energy sciences, electronics, optoelectronics and biological science. His discovery and breakthroughs in developing nanogenerators established the principle and technological road map for harvesting mechanical energy from environment and biological systems for powering personal electronics. His research on self-powered nanosystems has inspired the worldwide effort in academia and industry for studying energy for micro-nano-systems, which is now a distinct disciplinary in energy research and future sensor networks. He coined and pioneered the field of piezotronics and piezophototronics by introducing piezoelectric potential gated charge transport process in fabricating new electronic and optoelectronic devices. Details can be found at: http://www.nanoscience.gatech.edu.

**Di Wei** received his B.Sc. from the University of Science and Technology of China (USTC) and both his M.Sc. and Ph.D. from Åbo Akademi University in Finland. His research focuses on the applications of nanotechnology in energy and sensor systems. In this field, he has published over 120 papers in leading journals, including Nat. Energy, Nat. Commun., Sci. Adv., PNAS, Joule, Matter, Adv. Mater., Angew. Chem. Int. Ed., J. Am. Chem. Soc., Energ. Environ. Sci., Chem. Soc. Rev. etc. Wei holds a portfolio of over 200 international patents (including PCT filings), with nearly 100 successfully granted. Many of these patents have been transferred to leading companies such as Nokia in Finland and Lyten in the USA. Additionally, he has edited four English books published by Wiley and Cambridge University Press, among others. His contributions have been recognized with numerous accolades, including the First Prize of the Nokia Global Innovation and Excellence Award, the Brian Conway Prize in Physical Electrochemistry from the International Society of Electrochemistry (ISE), and various honors from ISE and the Royal Society of Chemistry (RSC). Details can be found at: http://www.iontronics.group/en/.